

Optimal design of a distributed energy resource system that economically reduces carbon emissions

Robert J. Flores*, Jacob Brouwer

Advanced Power and Energy Program, University of California, Irvine, CA 92617, United States

HIGHLIGHTS

- Analysis on minimum cost to reduce carbon emissions using optimization is explored.
- Novel utility rate, generator state, and transportation constraints are presented.
- The effect of export price of electricity is explored.
- The cost to reduce CO_{2e} emissions is determined for different technology scenarios.
- Optimal technology adoption trajectories are established for the same scenarios.

ARTICLE INFO

Keywords:

Mixed-integer linear program
Distributed energy optimization
Greenhouse gas reduction
Solar export rates

ABSTRACT

Distributed energy resources (DER) are commonly associated with reduced CO_{2e} emissions. The decision to design such a system that reduces emissions typically results in increased costs. In order to economically select and operate a DER system that also reduces CO_{2e} emissions, a mixed integer linear program for sizing and dispatching a DER system was developed and used with real data to determine the optimal DER design that reduces emissions at the lowest cost. The optimization program includes a novel formulation of constraints that govern utility natural gas, generator operation, and interaction with fleet vehicles. The results show that the least expensive way of reducing CO_{2e} is through the use of renewable gas in a conventional combined heat and power engine (i.e., a gas turbine), resulting in a cost to reduce emissions of between \$120 and \$150 per CO_{2e} tonne. Reducing emissions further requires the adoption of higher efficiency generators, or renewable generators, increasing cost of CO_{2e} by up to \$475 per tonne. Allowing for electrical export and the offset of grid operations results in the purchase of less energy storage, reducing the cost of CO_{2e} to \$190 per tonne under retail electricity rates, or \$230 per tonne when the DER operator sends excess renewables back to the utility grid for free. Finally optimization results for this particular case indicate that changes to the transportation system occur last since the marginal costs of changing fleet vehicles is highest versus the CO_{2e} reduction benefit.

1. Introduction

In 2013, the University of California system committed to "... emitting net zero greenhouse gases (GHG) from its buildings and vehicle fleets by 2025..." [1]. This commitment was made in support of California State Law aimed at reducing GHGs [2], and to address the "...growing environmental crisis..." created by climate change [1]. In order to reach this goal, the UC system is considering numerous on- and off-campus options aimed at reducing GHG emissions, including the use of solar power on- and off-campus, and the use of biogas fuel.

Ideally, the path towards carbon neutrality would simultaneously consider all University of California campuses, medical centers, and

national laboratories. However, major decisions are made at the campus level, and the resolution required for some decisions, such as the types and quantities of renewable distributed energy resources (DER) to adopt at each institution, require a more granular approach. DER includes distributed generation (DG), including small gas turbines (GT) and fuel cells (FC) with waste heat recovery through a heat recovery unit (HRU), solar photovoltaics (PV), combined with various types of electrical and/or thermal energy storage (EES and TES, respectively). Considering that many institutions and communities around the world also desire to reduce their GHG emissions in a cost-effective manner, it is important to understand the technology mixes that help reduce GHGs at the campus or community level for the lowest

* Corresponding author.

E-mail address: rjf@apep.uci.edu (R.J. Flores).

Nomenclature	
agg	aggregated
Bldg	building
Boil	boiler
cap	capital cost
chrg	charging (energy storage)
con	conventional vehicle
dchrg	discharging (energy storage)
ex	electrical export
DER	distributed energy resource
DERopt	distributed energy resource optimization
DG	distributed generation
EES	electric energy storage
EVSE	electric vehicle supply equipment
FC	fuel cell
GHG	greenhouse gas
GT	gas turbine
HRU	heat recovery unit
MILP	mixed integer linear program
ng	natural gas
NEM	net energy metering
OM	operations and maintenance
PEB	plugin electric bus
PV	photovoltaic
req	required
rng	renewable natural gas
SCE	Southern California Edison
SCG	Southern California Gas
TES	thermal energy storage
TOU	time of use
UC	unconstrained
UCI	University of California, Irvine
VC	vapor compression
veh	vehicle

possible cost.

Current literature presents numerous methods for DER system design and dispatch. Heuristic design and dispatch methods have been developed to use statistical [3] or physical models [4] to evaluate systems, design dynamic dispatch strategies [5,6], and to also quickly examine the performance of different DER system configurations in different climate zones [7–9]. Also, extensive DER system and dispatch work that uses optimization methods have been presented. Models using linear programming have been developed to optimize the design of DER systems [10–12], as well as DER system operation [13]. Linear formulations have also been proposed to minimize cost and GHGs associated with an energy demand while accounting for demand stochasticity and DER reliability [14].

One of the most popular methods for DER system design and operation optimization is mixed integer linear programming (MILP). This type of formulation can be used to capture the combination of discrete (i.e., number of generators purchased) and continuous (i.e., DG part load power setting) decisions that form a DER optimization problem. Dispatch models have been produced using MILP to minimize operating cost [15–17] and GHG emissions [16]. Prior MILPs that do not explicitly address GHG emissions account for the design of additional utility systems [18,19], legal constraints on DER system design [20], coproduction of chemicals [21], DG part load efficiencies [22], and renewable energy source [23] or electrical energy storage (EES) [24]. MILP formulations that include GHG emissions in the cost function [25–27], or as a constraint for limiting total emissions [28] have been presented. One popular and widely used formulation is known as the Distributed Energy Resource – Customer Adoption Model, which includes combined cooling heat and power components, renewable energy sources, EES, TES, electric vehicle interactions [29–37]. The cost function used by DER-CAM allows for minimization of cost, GHG emissions, or a combination of both through the use of weighting factors.

Finally, other nonlinear formulations have been presented that include DG part load efficiency [38–40] and nonlinear TES behavior [40]. Pruitt et al. [40] in particular, showed that optimal DER system design models can be improved through the inclusion of physical phenomena that affect DER operation. However, while the additional complexity generally produces more robust and realistic results, computational time is usually increased [40].

The current work expands upon prior DER system optimization work with the desire to address the University of California net zero GHG commitment. Since the focus of this work is DER technologies, some options, such as purchasing wholesale electricity from renewable sources (which are being evaluated by the University of California

[41]), are not addressed. Also, it is assumed that energy efficiency measures have already been widely implemented since these technologies tend to be cost-effective ways of reducing energy demand. For example, the University of California, Irvine campus has deployed deep energy efficiency measures to reduce demand by more than 50% [42].

In this work, a MILP called the Distributed Energy Resource optimization (DERopt) model is developed to minimize the cost of energy. DERopt includes a novel formulation for utility natural gas cost, TES, GT and FC operational state, and interaction with fleet vehicles, such as public transportation buses.

Solar PV systems, renewable gas, electrical export, and alternative fuel vehicles are considered for possibly reducing GHG emissions. The MILP is then exercised using real data for the University of California, Irvine (UCI) campus to determine the optimal DER system for adoption that minimizes cost while reducing GHG emissions.

2. Models

For the purpose of this work, all GHG emissions are quantified in terms of the equivalent amount of carbon dioxide emissions, CO₂ equivalent, or CO_{2e}.

2.1. UCI campus energy model

2.1.1. Central plant & building energy demand dynamics

A central cogeneration plant is currently operated at UCI to meet nearly all of the campuses electrical, heating, and cooling demands. The central plant consists of a 13.5 MW gas turbine, heat recovery steam generator, 5.5 MW steam turbine, eight vapor compression chillers that have a combined capacity of 16,680 tons of cooling, and a cold TES with 60,000 ton-hours of storage [43,44]. The central plant supplies hot and cold water to the campus through a district heating and cooling system that delivers energy to all of the major buildings on campus. In addition to the central plant, over 4 MW of solar PV has been installed across the campus.

Extensive monitoring equipment has been installed throughout the plant and across the campus. This monitoring capability has led to the collection of 15 min averaged electrical, heating, and cooling demand for the entire UCI campus from 2009 to the present. The amount of captured data would be difficult to directly use in the MILP proposed in Section 2.3. Instead, k-medoids clustering method that uses a similar structure to a typical facility location problem was built based on the work presented in [45] was built and used to filter the large set of data to a smaller, but representative data set. The filtering method reduces 12 months of 15 min data down to three months, allowing for the

generation of a tractable optimization model while maintaining the load dynamics that occur in 15 min data.

The extensive plant monitoring allows for the separation of electricity required to meet cooling demand, and electricity for all other end uses. As a result, the filtered electrical demand consists of only non-cooling loads, while the cooling demand represents the energy required to maintain the district cooling system. Likewise, heating demand represents the requirements of the district heating system. Demand data for the 2012 year was selected due to the completeness of the energy data. The resulting filtered data is shown in Fig. 1 and Table 1 contains summary values for the same data. Note that campus electrical demand is lower in the summer than the winter due to summer break.

2.1.2. Transportation demand

In addition to the campus energy demand, UCI maintains a fleet of vehicles used for a variety of purposes. Only campus fleet vehicles (not those used by employees or students for commuting) are considered in this work. More information on the fleet of buses and the bus system, known as the Anteater Express, can be found at the Anteater Express website [46].

Although the routes during the normal school year and summer differ, this work assumes that certain routes and route properties are constant. Route properties include the number of required buses, the cumulative length of each route, the time of arrival at the bus depot, and dwell time at the bus depot. Using these assumptions, the bus routes described in [46] have been condensed down to a set of routes described in Table 2.

Assuming that all buses on all routes are fueled using conventional fuels, and a bus operated using conventional fuel emits 1.15 kg CO₂e per mile, the Anteater Express is responsible for emitting 182 metric tons of CO₂e over three months of operation, a period of time that directly corresponds to the UCI campus energy demand shown in Fig. 1.

2.2. Utility cost and carbon emissions model

UCI is located in Southern California and falls within the service

Table 1

Summary of electrical, heating, and cooling demand for the filtered UCI campus energy demand data set.

Season	All	Summer	Winter
Average Electrical Demand (MW)	8.69	6.33	9.84
Max Electrical Demand (MW)	15.74	12.50	15.74
Electrical Load Factor	0.55	0.51	0.63
Average Heating Demand (MW)	9.84	7.18	11.14
Max Heating Demand (MW)	27.03	14.74	27.03
Heating Load Factor	0.36	0.49	0.41
Ratio of Heating to Electrical Load	1.13	1.14	1.13
Average Cooling Demand (MW)	13.17	20.16	9.75
Max Cooling Demand (MW)	45.08	45.08	44.70
Cooling Load Factor	0.29	0.45	0.22
Ratio of Cooling to Electrical Load	1.52	3.19	0.99

Table 2

Aggregated Anteater Express bus route data for input into DER optimization model.

Route	Range (Miles)	Required Vehicles	Time of Arrival at Base (Time)	Time at Base (Hours)
Arroyo Vista	136	2	21:00	10
Main	153	2	21:00	10
Newport/Park West	150	2	23:00	8
Vista Del Campo	101	3	19:00	12
Vista Del Campo Norte	107	3	19:00	12
Camino del Sol	108	2	19:00	12
American Campus Communities Combined	38	2	23:00	8

territory of Southern California Edison (SCE) for electricity and Southern California Gas (SCG) for natural gas. Although UCI receives electrical and natural gas service through special contracts, this work assumes that typical utility rates are used for both electricity and natural gas so that the results of the analyses can be more generally

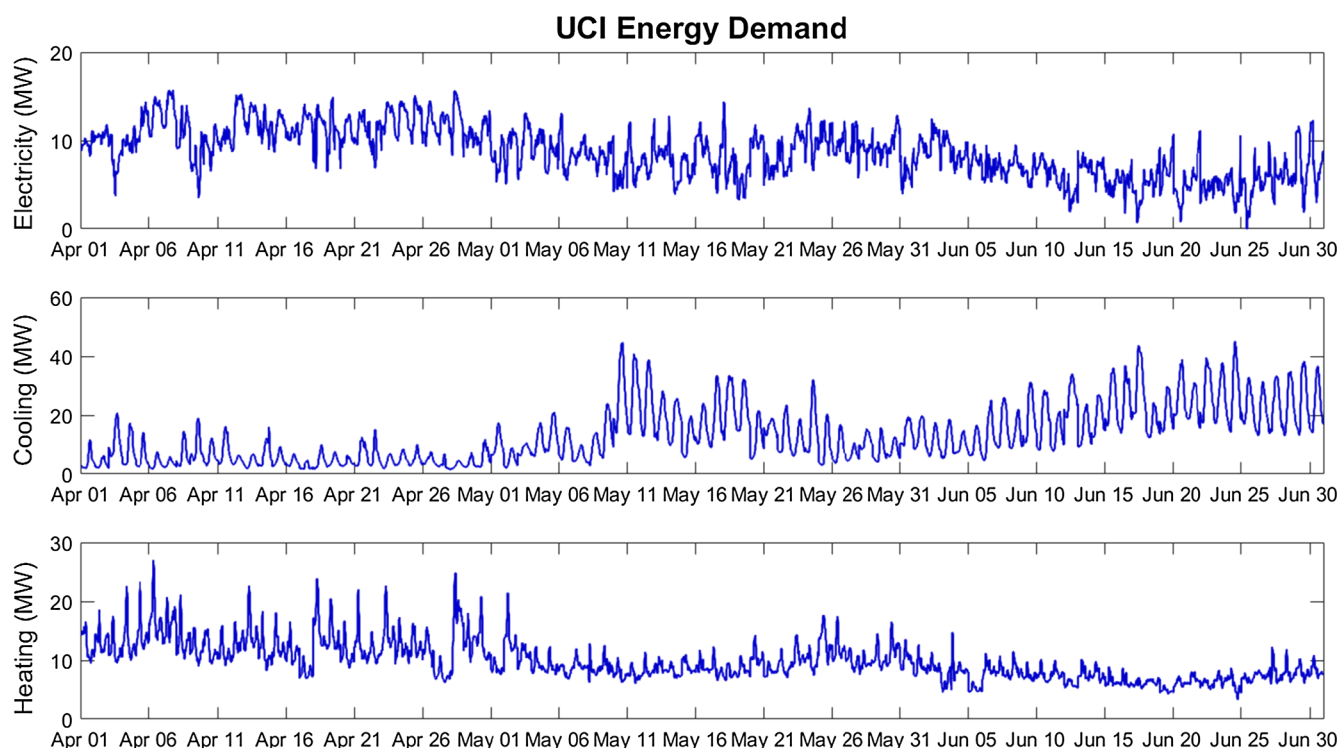


Fig. 1. Filtered UCI campus dynamic energy demand data.

applicable. Since this work considers both cost and GHG emissions, the utility models used in this study include the associated emissions.

2.2.1. Utility electricity

The applicable SCE rate for commercial and industrial customers with an electrical demand greater than 500 kW is TOU-8. Under TOU-8, seasonal demand and energy charges exist. A time of use (TOU) energy charge applies year round, with the highest energy costs occurring during the middle of the day. A non-TOU demand charge applies to all months, with TOU demand charges existing for on-peak and mid-peak during the summer and only on-peak during the winter. The SCE rate model is fully described in [5,6,47].

Typically, DER optimization studies that account for GHG emissions use average grid GHG emission factors that are similar to or exactly those presented in the Department of Energy eGrid database [48]. In reality, grid operation and the corresponding GHG emission factors change throughout the day. Instead of using an averaged emission factor, a time-resolved GHG emissions factor was developed for this work. The California Independent System Operator website [49] was used to determine the percent of total power delivered to California customers produced by carbon-free generating sources (renewable, geothermal, nuclear, hydro, etc.) for each one hour period for the year 2015. By making the assumption that the rest of the electricity was produced using natural gas-fired combined cycle power plants (a reasonably good assumption for California power generation), a time-resolved emissions factor was produced for California. This time-resolved emissions factor was then normalized to the average equivalent CO_{2e} emissions factor presented in [48]. The time-resolved emissions factor was then reduced to a representative set of winter and summer emissions using the same clustering method used to filter the building data [45]. Two weeks of the resulting emissions factor profiles for electricity purchased from a utility in California in summer and winter are shown in Fig. 2, where the x-ticks denote noon for each day. According to this model, the GHG emissions associated with each unit of electricity is lowest during the day, and highest at night. These dynamics are primarily associated with the fact that the California grid contains a high penetration of solar photovoltaic generation.

2.2.2. Utility natural gas

The applicable SCG natural gas rate has a declining block structure. Three natural gas blocks, or tiers, exist, each denoted by a level of monthly consumption. As a customer purchases natural gas from SCG, they move through the first tier, to the second, and to the third, with each tier having progressively lower cost natural gas. Assuming that natural gas consists only of methane, that any combustion occurring on the campus is complete, and that the boiler is 90% efficient, 5.78 kg CO_{2e} are emitted in order to supply one therm of heat to the campus.

2.3. DERopt model

The Distributed Energy Resource Optimization (DERopt) model is designed to find the least expensive combination of utility energy purchases, DER systems, bus fleet investments or other energy conversion, storage or conservation measures, together with operation (i.e., dispatch) of the resources to meet all energy demand with the constraint of reducing GHG emissions to a specific level [50]. The renewable energy sources included in this formulation are solar PV panels and renewable gas for use by DG and in a boiler. Since the system is being designed for a preexisting campus, it is assumed that a preexisting heating and cooling system exists that is sufficiently large to meet the campus thermal demand. Although energy efficiency measures may include adopting more efficient vapor compression chilling or boiler systems, these options are not included in the current formulation. Also, a power generation bottoming cycle, such as a steam turbine, is also not included in the current optimization. A schematic of the potential DER system is shown Fig. 3. Note that wind power is not included in the current work. Although renewable wind generation is critical to overall economic reduction of CO_{2e} emissions, this technology is not included in the current work since wind speeds are so low on the UCI campus [51]. However, if wind resources are sufficient elsewhere making wind power feasible, including this renewable resource can be achieved using a formulation similar to the solar resources as described in this section.

The sets, parameters, and decision variables that are used to describe the mixed integer linear program (MILP) that must be solved to accomplish the optimization are shown in the following subsections. The investment cost for each technology is converted into a monthly loan payment for all items considered in the optimization. The loan

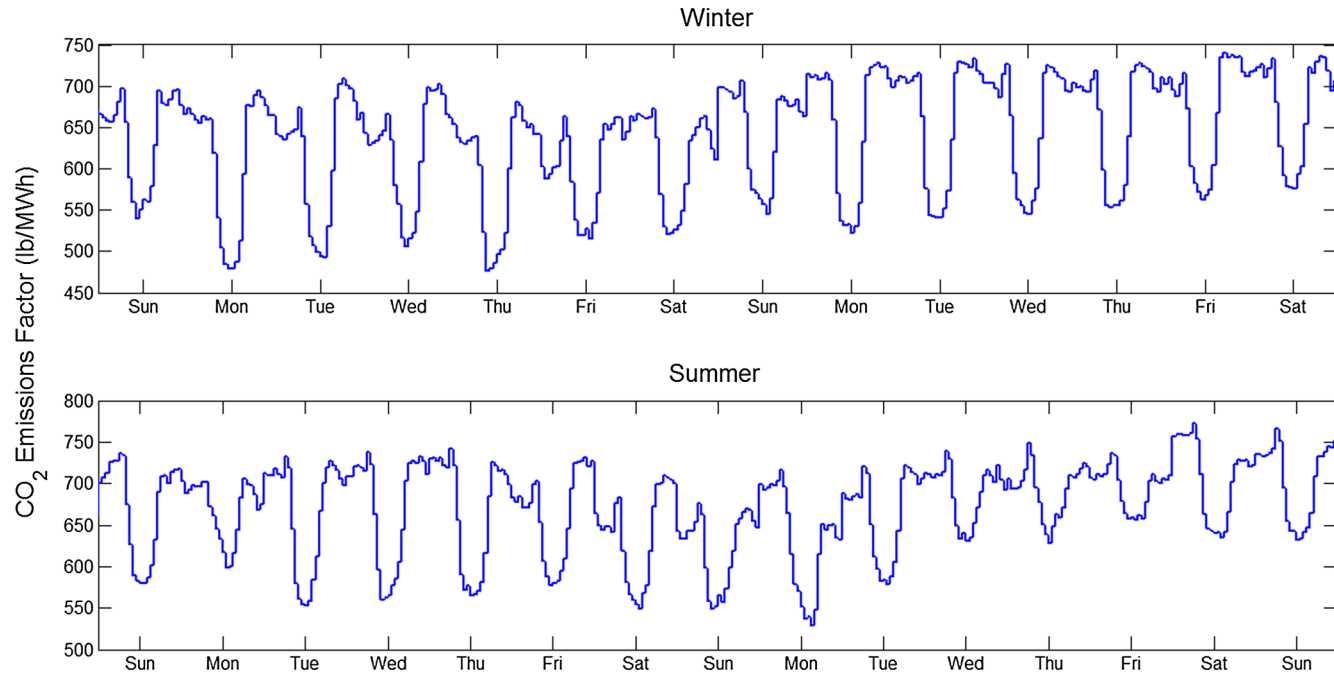


Fig. 2. Time-resolved CO_{2e} emissions factors for the State of California in 2015 during two winter weeks and two summer weeks.

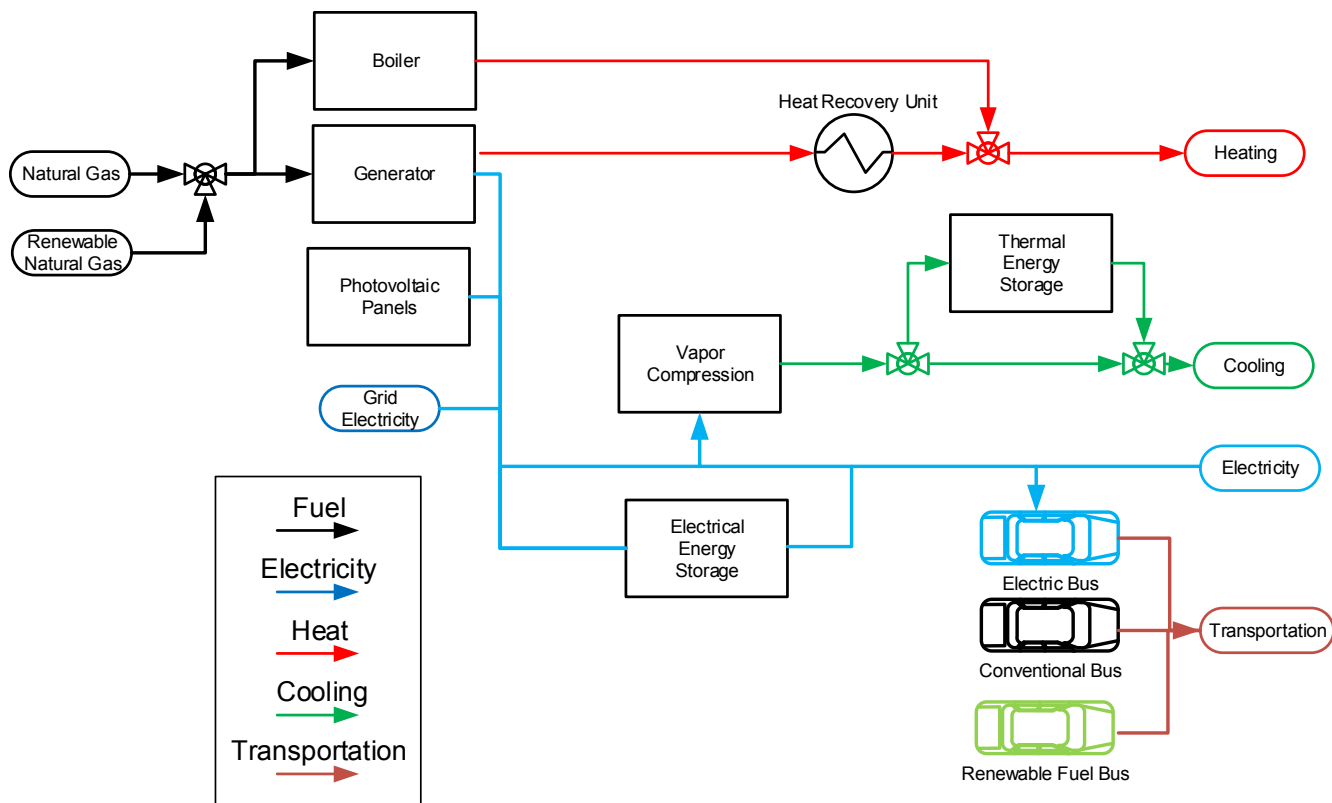


Fig. 3. Schematic of energy flows and DER systems to be optimized to meet campus heating, cooling, electricity, and fleet transportation demand dynamics.

payment amount, which accounts for finance, fixed operations and maintenance costs, etc., is the value that is used in the MILP, not the full purchase cost. The conversion factor between a therm and kWh occasionally appears as the constant $C_1 = 1 \text{ therm} / 29.3 \text{ kWh}$.

2.3.1. Sets

The sets shown below are only applicable to groups of things that are larger than one. For the purposes of this work, only one type of HRU, TES, EES, solar PV, or plugin electric bus (PEB) technology is included in the optimization, and these technologies do not receive a formal set description.

- $d \in D$: Set of all days in simulation
- $n \in N$: Set of all months
- $m \in M$: Set of all summer months ($M \subset N$)
- $h \in H_n$: Set of all 60 min increments in month n
- $t \in T_n$: Set of all 15 min increments in month n
- $\in O_m$: Set of all 15 min increments during on-peak in summer month m ($O \subset T$)
- $p \in P_m$: Set of all 15 min increments during mid-peak in summer month m ($P \subset T$)
- $k \in K$: Set of all generator types
- $r \in R$: Set of routes
- $y \in Y$: Set of conventional vehicles that can be purchased

2.3.2. Distributed generation

Two types of DG are considered for adoption: a 13.5 MW gas turbine (GT) and a 1 MW fuel cell (FC). Generator specific parameter values for the current work are presented below in Table 3, and generator decision variables are shown in Table 4.

2.3.3. Electrical and thermal energy storage systems

In the current formulations, both EES and TES use similar variables, although the physical interpretation is different. For example, both

have charging/discharging limits. For the EES, these limits are created by the size of the wires connecting the EES to the campus and the associated power electronics, whereas the TES limits are created by the size of the pipes and pumps that connect the TES to the district cooling system. Nevertheless, the parameters and decision variables are presented together, with the parameter values for the specific technologies shown in Table 5 and decision variables shown in Table 6.

2.3.4. Bus system

Bus system parameters can be split between route and vehicle parameters. Route parameters are:

- $n_{req,r}$ = Number of required vehicles for route r , *number of buses*, (Refer to Table 2).
- \bar{d}_r = Distance traveled on route r , *miles*, (Refer to Table 2).

Within available buses, parameters differ between PEB and

Table 3

DG technology parameters.

Parameter	Description	Units	GT Value	FC Value
$C_{cap, DG,k}$	Capital cost for DG of type k	\$/kW	1400	4000
$S_{DG,k}$	Rate power for DG of type k	MW	13.5	1
$C_{om, DG,k}$	O&M cost for DG of type k	\$/kWh	0.01	0.023
$C_{start, DG,k}$	Startup cost for DG of type k	\$/start	100	100
$\eta_{DG,k}$	Electrical efficiency for DG of type k	%	32	47
$\bar{\eta}_{DG,k}$	Maximum fuel utilization for DG of type k	%	90	90
$\delta_{DG,k}$	Minimum turndown for DG of type k	%	60	50
$\bar{\mu}_{DG,k}$	Maximum ramp-up rate for DG of type k	%/15 min	50	10
$\mu_{DG,k}$	Maximum ramp-down rate for DG of type k	%/15 min	50	10

Table 4
DG Decision Variables.

Decision Variable	Description	Units	Variable Type
$N_{DG,k}$	Number of DG of type k purchased	Generator units	Integer
$n_{DG\ on,k,h}$	Number of active DG of type k during hour h	Generator units	Integer
$n_{DG\ Start,k,h}$	Number of DG of type k starting up during hour h	Generator units	Integer
$e_{DG,k,t}$	Energy output from DG of type k during time t	kWh	Continuous
$g_{DG,k,t}$	Natural gas consumption by DG k during time t	kWh	Continuous
$g_{rDG,k,t}$	Renewable gas consumption by DG k during time t	kWh	Continuous

combustion based buses. PEB parameters are:

- C_{EVSE} = Capital cost of electric vehicle supply equipment (EVSE), \$, (10,000).
- $\eta_{PEB\ mpkWh}$ = Electricity used by PEB during travel, miles/kWh, (2.1).
- S_{PEB} = Number of EVSE refueling for PEB, number of refueling ports, (2)
- S_{EVSE} = Power rating of EVSE, kW, (30)

Two conventional bus types are considered: one that uses conventional fuel, and another that uses renewable fuel. Parameters and decision variables for any combustion-based bus are described using the same type of parameters, decision variables, and constraints. Parameters for conventional vehicles are shown in Table 7. Decision variables for the bus system are shown in Table 8.

2.3.5. Campus demand and additional technologies

Parameters and decision variables associated with the campus energy demand and utilities are shown in Table 9 and Table 10 respectively.

Parameters and decision variables for all other technologies are shown in Table 11 and Table 12. These technologies include new technologies (solar PV and HRU) and legacy technologies (boiler and vapor compression (VC)). This work assumes that a boiler for heating and VC for cooling exists on the UCI campus already (as is the case for many campuses or other sites that may want to design and operate energy infrastructure to reduce costs and GHG emissions).

2.3.6. Problem formulation

The proposed cost function for the MILP formulation is shown in Equation (1) below, and includes the purchased utility electricity and natural gas, DER investment and operating cost, and the operations cost associated with the preexisting heating and cooling technologies.

Table 5
EES/TES Technology Parameters.

Parameter	Description	Units	EES Value	TES Value
$C_{cap\ EES}, C_{cap\ TES}$	Capital cost of EES/TES	\$/kWh	200	50
$C_{om\ EES\ chrg}, C_{om\ TES\ chrg}$	Cost to charge EES/TES	\$/kWh	0.001	0.001
$C_{om\ EES\ dchrg}, C_{om\ TES\ dchrg}$	Cost to discharge EES/TES	\$/kWh	0.001	0.001
$\alpha_{EES}, \alpha_{TES}$	Retained EES/TES storage between 15 min periods	%	99.9	99.9
$\eta_{EES\ chrg}, \eta_{TES\ chrg}$	EES/TES charging efficiency	%	95	95
$\eta_{EES\ dchrg}, \eta_{TES\ dchrg}$	EES/TES discharging efficiency	%	95	95
$\delta_{EES}, \delta_{TES}$	Maximum EES/TES state of charge	% of purchased capacity	95	99
$\delta_{-EES}, \delta_{-TES}$	Minimum EES/TES state of charge	% of purchased capacity	10	5
$\bar{\mu}_{EES}, \bar{\mu}_{TES}$	Maximum EES/TES charging rate	% of purchased capacity	25	25
μ_{-EES}, μ_{-TES}	Maximum EES/TES discharging rate	% of purchased capacity	25	25

Table 6
EES/TES Decision Variables.

Decision variable	Description	Units	Variable Type
$e_{EES\ size}, e_{TES\ size}$	EES/TES purchased	kWh	Continuous
$e_{EES\ chrg,t}, e_{EES\ chrg,t}$	Energy charged to EES/TES during time t	kWh	Continuous
$e_{EES\ dchrg,t}, e_{EES\ dchrg,t}$	Energy discharged to EES/TES during time t	kWh	Continuous

$$\begin{aligned}
 & \text{minimize} \quad \sum_t C_{grid,t} e_{grid,t} + \sum_n C_{DC,n} P_{max,n} + \sum_m C_{on\ DC,m} P_{on\ max,m} \\
 & + \sum_m C_{mid\ DC,m} P_{mid\ max,m} + \sum_n C_{ng,n} + C_{rng,n} e_{rng} \\
 & + \sum_k C_{cap\ DG,k} S_{DG,k} N_{DG,k} + \sum_k \sum_t C_{om\ DG,k} e_{DG,k,t} \\
 & + \sum_k \sum_h C_{start\ DG,k} n_{DG\ start,k,h} + C_{cap\ HRU} P_{maxHRU} \\
 & + \sum_t C_{om\ HRU} e_{HRU,t} + C_{cap\ PV} P_{maxPV} + \sum_t C_{om\ PV} e_{PV} \\
 & + C_{cap\ EES} E_{EES} + \sum_t C_{om\ EES\ dchrg} e_{EES\ chrg} \\
 & + \sum_t C_{om\ EES\ chrg} e_{EES\ hrz} + C_{cap\ TES} E_{TES} \\
 & + \sum_t C_{om\ TES\ dchrg} e_{TES\ chrg,t} + \sum_t C_{om\ TES\ chrg} e_{TES\ dchrg,t} \\
 & + \sum_t C_{om\ VC} e_{VC,t} + \sum_t C_{om\ Boil} e_{boil,t} + \sum_t C_{om\ Boil\ r} e_{boil\ rng,t} \\
 & - \sum_t C_{ex,t} e_{ex,t} + \sum_r \left(C_{PEB} n_{PEB,r} + \sum_y C_{con,y} n_{con,y,r} \right) + C_{EVSE} n_{EVSE} \quad (1)
 \end{aligned}$$

The constraints associated with (1) ensure that all energy requirements are met within the physical and operational constraints of all adopted and preexisting technologies. Constraint (2) ensures that the electrical demand created by the campus, VC chiller operation, EES charging, PEB refueling, and export to the grid is met by electricity purchased from the grid, produced by adopted DG, or EES discharge. Constraint (3) ensures that the campus heating load is met by either heat captured from DG through the HRU, or by the boiler. Constraint (4) ensures that the campus cooling demand and charging of the TES is met by cooling produced from VC chiller operation or discharging of the TES.

$$\begin{aligned}
 e_{grid,t} + \sum_k e_{DG,k,t} + e_{pv,t} + e_{EESdchrg,t} &= E_{BldgElec,t} + \frac{e_{VC,t}}{COP_{VC}} + e_{EESchrg,t} \\
 + e_{v_r,agg,t} + e_{ex,t} & \quad (2)
 \end{aligned}$$

$$e_{HRU,t} + e_{boil,t} + e_{boilrng,t} = E_{BldgHeat,t} \quad (3)$$

$$e_{VC,t} + e_{TESdchrg,t} = E_{BldgCool,t} + \left(1 + \frac{\Delta T_{bldg-1}}{\Delta T_{2-bldg}} \right) e_{TESchrg,t} \quad (4)$$

Constraints (3) and (4) are applied to the district heating and

Table 7
Conventional vehicle parameters.

Parameter	Description	Units	Convention Vehicle	Renewable Vehicle	PEB
$C_{vehCAP,y}/PEB$	Capital cost for vehicle y or PEB	\$/bus	500,000	700,000	1,200,000
$C_{vehOM,y}/PEB$	Operation cost for vehicle y or PEB	\$/Mile	0.20	0.60	0.01
$C_{con,y,r}/C_{PEB,r}$	Capital and operations cost of conventional vehicle y or PEB, operated on route r	\$	$\text{loan}(C_{vehCAP,y}/PEB)$ + size (D)* $\bar{d}_r*C_{vehOM,y}/PEB$		
$C_{conCO_2,y}$	CO _{2e} emissions for conventional vehicle y	Kg CO _{2e} /mile	1.15	0.12	n/a

Table 8
Vehicle decision variables.

Decision Variable	Description	Units	Variable Type
$n_{PEB,r}$	Number of purchased PEBs for route r	Number of buses	Integer
n_{evse}	Number of purchased EVSE	Number of EVSE	Integer
$PEB_{refuel,r,t}$	Electricity sent to electric buses purchased for route r, at time t	kWh	Continuous
$ev_{r,agg,t}$	Aggregated PEB refueling load at time t	kWh	Continuous
$n_{con,y,r}$	Number of conventional vehicle y, for route r	Number of buses	Integer

cooling loop operation at UCI. The physical connection between the serviced buildings and the district heating system is an individual heat exchanger installed at each location, allowing for energy transfer between the campus loop and each building. For the TES to provide cooling to the campus buildings, the useful storage must be maintained at a temperature lower than the highest temperature in the building side of each heat exchanger. Otherwise, the direction of energy flow from the building to the district cooling system through the heat exchanger would be reversed. If the stored cold water leaves the TES tank at T_2 , and the maximum temperature on the building side of the heat exchanger is T_{bldg} , then the useful thermal energy is only associated with the difference in temperatures $T_{bldg} - T_2$, represented as the parameter ΔT_{2-bldg} . When the cold storage water leaves the building, travels through the district cooling loop, arriving at the central plant at a higher temperature T_1 , ($T_1 > T_{bldg}$), then the cold return water must be chilled to T_{bldg} before useful thermal energy can be stored. Then the actual cooling energy input into the TES is the sum of the useful storage

and the energy required to achieve a temperature where the storage is useful. This can be expressed by $(\Delta T_{2-bldg} + \Delta T_{bldg-1})/\Delta T_{2-bldg}$, or $1 + (\Delta T_{bldg-1}/\Delta T_{2-bldg})$.

The maximum utility demands used to determine each of the peak demand charges are determined with constraints (5) through (7). Constraint (5) governs the non-TOU demand charges, while constraints (6) and (7) govern on-peak and mid-peak TOU demand charges.

$$4e_{Grid,t} \leq P_{max,n} \quad (5)$$

$$4e_{Grid,o} \leq P_{onmax,m} \quad (6)$$

$$4e_{Grid,p} \leq P_{midmax,m} \quad (7)$$

Only monthly utility natural gas costs are accounted for in (1). Due to the nature of the declining block natural gas rate structure, the cost of natural gas can be modeled as a piece-wise continuous function of total monthly consumption [54]. By separating the line segments by the tiers (0 to 250, 250 to 4167, and 4167 to an arbitrary limit of therms per month) a linear piece-wise function can be constructed that perfectly captures utility gas costs, which can be used in a MILP [55]. By introducing a new set of variables, $\lambda_{i,n}$, the total cost and total level of consumption can be determined in constraints (8) and (9), respectively. The set of variables $\delta_{j,n}$ are then introduced and used in constraints (11) through (15) to ensure that the campus progresses through each individual tier as utility gas purchases accrue each month. The formulation that was implemented for DG capital cost is similar to the current natural gas cost formulation which is presented by Liu et al. [21].

$$0\lambda_{1,n} + T_1\lambda_{2,n} + T_2\lambda_{3,n} + T_3\lambda_{4,n} = \sum_t \frac{C_1 e_{boil,t}}{\eta_{boil}} + \sum_k \sum_t C_{1g} g_{DG,k,t} \quad (8)$$

$$C_{ng,n} = 0\lambda_{1,n} + C_{ng,n,1}\lambda_{2,n} + C_{ng,n,2}\lambda_{3,n} + C_{ng,n,3}\lambda_{4,n} \quad (9)$$

$$\lambda_{1,n} + \lambda_{2,n} + \lambda_{3,n} + \lambda_{4,n} = 1 \quad (10)$$

Table 9
Building and Utility Parameters.

Parameter	Description	Units	Value
$E_{Bldg\ Elec,t}$, $E_{Bldg\ Heat,t}$, $E_{Bldg\ Cool}$, $A_{PV\ Area}$	Electrical, heating, and cooling demand at time t	kWh	Refer to Fig. 1
$e_{solar,t}$	Area available for solar PV installation	m ²	10,000,000
ΔT_{bldg-1}	Average available insolation at time t	kWh/m ²	Taken from [52]
ΔT_{2-bldg}	Difference in temperature between the heat exchanger providing cooling to the building and the temperature of the used storage working fluid	°C	3
CO_2Limit	Difference in temperature between the charged thermal energy storage working fluid and the heat exchanger providing cooling to the building	°C	5
$C_{grid,t}$	Greenhouse gas emissions limit applied to DER system design	kg	Varies
$C_{DC,n}$	Electrical utility energy charge at time t	\$/kWh	Refer to [53]
$C_{onDC,m}$	Non-TOU demand charge in month n	\$/kW	14.88
$C_{midDC,m}$	On-peak demand charge in summer month m	\$/kW	23.74
T_1, T_2, T_3	Mid-peak demand charge in summer month m	\$/kW	6.55
$C_{ng,n,1}, C_{ng,n,2}, C_{ng,n,3}$	Tiered levels of consumption according to the natural gas rate structure	Therms	250, 4167, 150,000
$C_{ng,n}$	Cost of natural gas during month n at the levels of monthly consumption defined by T_1, T_2, T_3	\$	222, 2690, 69,800
$C_{ex,t}$	Cost of renewable gas during month n	\$/kWh	0.034, which is \$1/therm
	Price at which electrical utility purchases energy from the building at time t	\$/kWh	Energy charge $C_{grid,t}$ minus transmission and distribution cost
$C_{CO_2Grid,t}$	CO _{2e} emissions associated with utility electricity at time t	kg CO _{2e} /kWh	Refer to Fig. 2
C_{CO_2NG}	CO _{2e} associated with natural gas use	kg CO _{2e} /therm	5.78
C_{CO_2RNG}	CO _{2e} associated with renewable gas use	kg CO _{2e} /therm	0.91

Table 10
Utility decision variables.

Decision Variable	Description	Units	Variable Type
$e_{grid,t}$	Electricity purchased from grid at time t	kWh	Continuous
$P_{max,n}$	Maximum demand during month n	kW	Continuous
$P_{on\ max,m}$	Maximum on-peak demand during summer month m	kW	Continuous
$P_{mid\ max,m}$	Maximum mid-peak demand during summer month m	kW	Continuous
$C_{ng,n}$	Cost of natural gas purchased during month n	\$	Continuous
$\lambda_{i,n}$	i component of piece-wise function of natural gas cost for month n	n/a	Continuous
$\delta_{j,n}$	j component to impose special order set type 2 constraint of natural gas piece-wise function for month n	n/a	Binary
e_{rng}	Renewable gas purchased	Therms	Continuous
$e_{ex,t}$	Electricity sold back to the grid at time t	kWh	Continuous

Table 11
Additional technology parameters.

Parameter	Description	Units	Value
$C_{cap\ HRU}$	Capital cost for HRU	\$/kW	100
$C_{om\ HRU}$	O&M cost for HRU	\$/kWh	0.001
ε_{HRU}	Effectiveness of HRU	%	90
$C_{cap\ PV}$	Capital cost for solar PV system	\$/kW	2000
$C_{om\ PV}$	O&M Cost for solar PV system	\$/kWh	0.001
η_{PV}	Photovoltaic efficiency at nominal conditions	%	20
$C_{om\ VC}$	Vapor compression chiller O&M cost	\$/kWh	0.014
COP_{VC}	Coefficient of performance for VC chiller	Cooling out/work in	3.4
$C_{om\ Boil}$	Boiler O&M cost	\$/kWh	0.001
η_{Boil}	Boiler efficiency	%	90

Table 12
Additional technology parameters.

Decision variable	Description	Units	Variable Type
$P_{max\ HRU}$	Size of adopted HRU	kW	Continuous
$e_{HRU,t}$	HRU output during time t	kWh	Continuous
P_{pv}	Solar PV system size purchased	kW	Continuous
$e_{pv,t}$	Solar PV system output during time t	kWh	Continuous
$e_{vc,t}$	VC Chiller output at time t	kWh	Continuous
$e_{boil,t}, e_{boil\ rng,t}$	Boiler output using utility and renewable gas at time t	kWh	Continuous

$$\lambda_{1,n} - \delta_{1,n} \leq 0 \quad (11)$$

$$\lambda_{2,n} - \delta_{1,n} - \delta_{2,n} \leq 0 \quad (12)$$

$$\lambda_{3,n} - \delta_{2,n} - \delta_{3,n} \leq 0 \quad (13)$$

$$\lambda_{4,n} - \delta_{3,n} \leq 0 \quad (14)$$

$$\delta_{1,n} + \delta_{2,n} + \delta_{3,n} = 1 \quad (15)$$

In addition to having the option to purchase utility natural gas, the campus also has the option to purchase renewable gas that is delivered through the natural gas system. It is assumed that the campus will pay a flat fee for the renewable gas, and that total renewable gas consumption is the sum of the gas use in all of the individual gas consuming technologies. The total consumption of renewable gas is governed by constraint (16).

$$\sum_k \sum_t g_{rDG,k,t} + \sum_t \frac{e_{boil\ rng,t}}{\eta_{Boil}} = e_{rng} \quad (16)$$

Constraints (17) through (23) govern the operation of any adopted natural gas fired generators. Constraint (17) limits the number of active generators by the number of purchased units. Constraint (18) sets the consumption of both utility and renewable gas to be proportional to the electrical production. Constraint (19) establishes when a generator is started. Constraint (20) limits the electrical output by the number of active generators during any time period. Constraint (21) establishes

the minimum power output by any of the active generators. Constraints (22) and (23) limit the ramping ability of each active generator.

$$n_{DGon,k,h} \leq N_{DG,k} \quad (17)$$

$$\eta_{DG,k} g_{DG,k,t} + \eta_{DG,k} g_{rDG,k,t} = e_{DG,k,t} \quad (18)$$

$$n_{DGon,k,h} - n_{DGon,k,h-1} \leq n_{DGstart,k,h} \quad (19)$$

$$e_{DG,k,t} \leq S_{DG} n_{DGon,h} \quad (20)$$

$$\delta_{DG,k} S_{DG,k} n_{DGon,k,h} \leq e_{DG,k,t} \quad (21)$$

$$e_{DG,k,t} - e_{DG,k,t-1} \leq \bar{\mu}_{DG,k} S_{DG,k} n_{DGon,k,h} \quad (22)$$

$$e_{DG,k,t-1} - e_{DG,k,t} \leq \mu_{DG,k} S_{DG,k} n_{DGon,k,h} \quad (23)$$

Constraints (17) through (23) do not explicitly require that a generator be operated or shut down for a specific period after a change in operational state. However, the aggregated power variable is determined for each 15 min, while the active generator variable is determined on an hourly basis, thus eliminating any rapid on-off-on dispatch as prescribed by the optimization. Mandatory on- or off-time constraints have been presented in the literature for determining optimal operation after a DER system has been sized, but these constraints require three times the number of integer variables associated with the state of each generator at each time step [16]. By separating the active generator and aggregated power output time scales, undesirable optimization results can be avoided. In addition, the current formulation reduces the number of integer decision variables, decreasing the overall complexity and time to solve the model. If desired, the active generator time scale can be increased to govern operation for entire peak periods when the determined adoption and operation of technologies that may be sensitive to on-off behavior, such as is the case for high-temperature fuel cell systems, which are typically operated continuously. While some optimality is sacrificed through this approach, the program benefits from implicitly including practical and realistic DG operation requirements while reducing the number of integer variables.

The adoption and operation of solar PV are governed by constraints (24) through (26). Constraint (24) and (25) limits the output from the PV panels to the amount of available insolation and adopted system size respectively. Constraint (26) limits the size of any adopted system by the area available for PV installation.

$$e_{pv,t} \leq e_{solar,t} \frac{P_{pv}}{\eta_{pv}} \quad (24)$$

$$4e_{pv,t} \leq P_{pv} \quad (25)$$

$$\frac{P_{pv}}{\eta_{pv}} \leq A_{PVArea} \quad (26)$$

Constraint (27) limits the thermal energy captured by the HRU to the size of the HRU adopted, while constraint (28) limits HRU output to the amount of available heat produced by the natural gas-fired DG.

$$e_{HRU,t} \leq P_{\max HRU} \quad (27)$$

$$\frac{e_{HRU,t}}{e_{HRU}} \leq \sum_k \frac{\bar{\eta}_{DG,k} - \eta_{DG,k}}{\eta_{DG,k}} e_{DG,k,t} \quad (28)$$

Constraints (29) through (32) govern the operation of the EES, while constraints (33) through (38) govern the operation of the TES. Constraints (29) and (34) are the energy balances for the respective storage technology, relating the current state of charge (SOC) to the prior SOC, plus charging, minus discharging. Constraints (30) and (31) for the EES and constraints (35) and (36) for the TES set the maximum and minimum SOC for the adopted storage technology and size. Constraints (32) and (33) for the EES and constraints (37) and (38) for the TES limit the rate at which the storage can be either discharged or charged.

$$e_{EESstore,t} = \alpha_{EES} e_{EESstore,t-1} + \eta_{EESchrg} e_{EESchrg,t} - \frac{e_{EESdchrg,t}}{\eta_{EESdchrg,t}} \quad (29)$$

$$e_{EESstore,t} \leq \bar{\delta}_{EES} e_{EESsize} \quad (30)$$

$$e_{EESstore,t} \geq \delta_{EES} e_{EESsize} \quad (31)$$

$$e_{EESdchrg,t} \leq \bar{\mu}_{EES} e_{EESsize} \quad (32)$$

$$e_{EESchrg,t} \leq \mu_{EES} e_{EESsize} \quad (33)$$

$$e_{TESstore,t} = \alpha_{TES} e_{TESstore,t-1} + \eta_{TESchrg} e_{TESchrg,t} - \frac{e_{TESdchrg,t}}{\eta_{TESdchrg,t}} \quad (34)$$

$$e_{TESstore,t} \leq \bar{\delta}_{TES} e_{TESsize} \quad (35)$$

$$e_{TESstore,t} \geq \delta_{TES} e_{TESsize} \quad (36)$$

$$e_{TESdchrg,t} \leq \bar{\mu}_{TES} e_{TESsize} \quad (37)$$

$$e_{TESchrg,t} \leq \mu_{TES} e_{TESsize} \quad (38)$$

Constraints (39) through (43) govern the adoption of fleet vehicles.

Constraint (39) ensures that the required number of vehicles for each route is purchased. Constraint (40) states that the amount of electricity delivered to any purchased PEB while the bus is parked at the base must equal the amount required to complete the applicable route. Constraint (41) aggregates the recharging of all PEBs for all routes into a single variable that is input into constraint (2). Constraint (42) ensures that the aggregated refueling of PEBs is limited by the combined capacity of adopted EVSE. Constraint (43) limits the number of adopted EVSE to the number of recharging ports on the purchased PEBs.

$$n_{PEB,r} + \sum_y n_{con,y,r} = n_{req,r} \quad (39)$$

$$\sum_{t \in day} PEB_{refuel,r,t} = \frac{\bar{d}_r}{\eta_{evmpkWh,l}} n_{PEB,r} \quad (40)$$

$$ev_{r,agg,t} = \sum_r PEB_{refuel,r,t} \quad (41)$$

$$ev_{r,agg,t} \leq \sum_n S_{evse,n} n_{evse,n} \quad (42)$$

$$n_{evse} \leq \sum_r S_{PEB} n_{ev,r} \quad (43)$$

Constraint (44) is the GHG emissions limit, and includes emissions from any emitting source, minus any GHG offset due to the export of electricity.

$$\sum_t C_{CO2grid,t} e_{grid,t} + \sum_n C_{CO2NG} (0\lambda_{1,n} + T_1\lambda_{2,n} + T_2\lambda_{3,n} + T_3\lambda_{4,n})_n + C_{CO2NG} e_{mg} + \sum_r \sum_y C_{con,y,r} \bar{d}_r n_{con,y,r} - \sum_t C_{CO2grid,t} e_{ex,t} \leq CO2Limit \quad (44)$$

3. DER system scenarios

Six different technology scenarios are considered. The baseline scenario includes the option to adopt a GT, FC, HRU, and solar PV. Three energy storage scenarios (EES, TES, EES+TES) allow for adoption of all technologies included in the baseline scenario plus the energy

Table 13
Optimal DER adoption of discrete technologies.

Gas Turbine (13.5 MW)												
CO _{2e} Reduction	UC	0%	33%	67%	80%	85%	87.5%	90%	92.5%	95%	97.5%	100%
Baseline	1	1	1	1	1	0	0	X	X	X	X	X
EES	1	1	1	1	1	1	0	0	0	0		
TES	1	1	1	1	1	1	0	0	X	X	X	X
EES+TES	1	1	1	1	1	1	0	0	0			
Export	1	1	1	1	1	1	1	1	1	1	1	1
Export w/EES+TES	1	1	1	1	1	1	1	1	1	1	1	1
Fuel Cell (1 MW)												
Baseline	0	0	0	0	0	13	14	X	X	X	X	X
EES	0	0	0	0	0	0	12	9	10			
TES	0	0	0	0	0	2	13	13	X	X	X	X
EES+TES	0	0	0	0	0	0	12	11	10			
Export	0	0	0	0	0	0	0	0	0	0	0	0
Export w/EES+TES	0	0	0	0	0	0	0	0	0	0	0	0
Vehicle Type (Conventional/Renewable)												
Baseline	14/0	14/0	14/0	14/0	8/6	4/10	0/14	X	X	X	X	X
EES	14/0	14/0	14/0	14/0	14/0	0/14	0/14	0/14	0/14			
TES	14/0	14/0	14/0	14/0	14/0	0/14	0/14	0/14	X	X	X	X
EES+TES	14/0	14/0	14/0	14/0	14/0	0/14	0/14	0/14	0/14			
Export	14/0	14/0	14/0	14/0	14/0	14/0	14/0	14/0	14/0	14/0	14/0	14/0
Export w/EES+TES	14/0	14/0	14/0	14/0	14/0	14/0	14/0	14/0	14/0	14/0	14/0	14/0

storage technology used as the scenario label. The export scenario includes all baseline scenario options, but allows for electrical export to occur. The final scenario includes all technologies included in the EES & TES scenario, and allows electrical export.

The CO_{2e} constraint implemented for each technology scenario by establishing the baseline that is based upon the emissions associated with campus operations when all energy needs are met by using utility electricity to meet all electrical and cooling demand, natural gas in a boiler to meet all heating demand, and conventional vehicles to meet all transportation demand. Under this scenario, 12,929 metric tons of CO_{2e} are emitted during the three months shown in Fig. 1.

For each technology scenario, the optimal DER was first determined using the optimization model described in Section 2.3 without a CO_{2e} emission constraint, labeled the unconstrained (UC) case. The CO_{2e} emission constraint was activated during subsequent optimization executions, with the allowable net CO_{2e} emission limit decreasing until either the problem was infeasible, or net emissions were zero.

For the scenarios that included electrical export, three separate scenarios were considered. First, rates consistent with current net energy metering (NEM) prices were included. Under NEM, a utility customer who exports excess electricity back to the utility receives a credit priced at the time of use retail cost of electricity, less transmission and distribution costs (approximately \$0.02 per kWh) [56]. In California, NEM retail rates are only applicable up to the quantity of electrical energy imported by the customer, and excess export is credited to the utility customer at wholesale electricity rates [57]. Instead of modeling this transition from NEM to wholesale price, a separate constant export price of \$0.03 per kWh (reasonable wholesale price) was considered in these periods. The final export price considered in this work is \$0 per kWh, or the utility customer receives no credit or payment for electrical export. Note that all results, except for those presented in Section 4.3, were determined using NEM rates. The validity of the use of NEM rates, and results for wholesale rates are assessed in Section 4.3.

This work assumes that 20% of the capital cost of all equipment is paid by the system adopter, and that the remaining 80% of the capital cost is financed through a loan with an annual interest rate of 8% and ten year life of the loan.

4. DER system optimization results

Optimal DER technology and vehicle adoption for all six technology scenarios is shown in Table 14 and Table 14, for all levels of CO_{2e} emissions reduction considered. Using the current optimization model, the only technology scenarios that could achieve a 100% net CO_{2e} emissions reduction included electrical export. Otherwise, a CO_{2e} emissions reduction beyond 87.5% for the baseline scenario, 90% for the TES scenario, and 92.5% for the EES and EES + TES scenario were found to be infeasible. These infeasible conditions are indicated in Table 14 and Table 14 by crossed out table entries.

According to the results, the optimal DER system for all technology scenarios is nearly identical when emissions are uncontrolled, or reduced by up to 67%. This shared system is comprised of a GT/HRU core, approximately three MW of PV (0% to 67% emission reduction only), and, when allowed, low levels of storage. Note that all scenarios that include storage experience a decrease in storage adoption when comparing the unconstrained emissions case to a 0% reduction. This is due to the lower than 100% round-trip efficiency associated with storage, and the ability of the existing and adopted systems to instantaneously meet the campus energy demand at all times.

Although the base technologies do not substantially change, the proposed system is capable of reaching an emissions reduction of 67%. This is achieved through the purchase of renewable gas (shown in Fig. 4), and operational changes (presented in Fig. 5). Optimal renewable and total natural gas purchases for the entire year are shown in Fig. 4, while Fig. 5 shows the source of electricity for all technology scenarios. Although all six technology scenarios are different, the operational results between similar scenarios were nearly identical, and are grouped together in both Fig. 4 (EES, TES, and EES + TES, are grouped as “energy storage only”, and export, and export w/EES + TES as “all export”), and Fig. 5 (EES with EES + TES, and export with export w/EES + TES). Both Fig. 4 and Fig. 5 show that emissions are reduced by up to 67% by increasing utility imports, and by replacing non-renewable fuel with renewable fuel. Although the fuel consumption for the baseline scenario and energy storage only scenarios in Fig. 4 appears to be similar in shape, baseline fuel consumption is lower by approximately 50,000 to 100,000 MMBtu per year when emissions are

Table 14
Optimal DER adoption of continuous technologies.

HRU (MW)										
Baseline	14.5	14.8	14.8	15.6	17.1	10.7	11.5	X	X	X
EES	14.6	15.4	15.4	15.4	16.7	17.1	9.9	7.4	8.2	
TES	14.5	15.3	15.3	15.3	16.7	16.5	10.7	10.7		
EES+TES	14.6	15.4	15.4	15.4	16.7	17.1	9.9	9.1	8.2	
Export	14.6	15.4	15.4	15.4	16.7	16.6	16.6	16.6	16.5	16.5
Export w/EES+TES	14.6	15.4	15.4	15.4	16.6	16.7	16.6	16.6	16.6	16.5
PV (MW)										
Baseline	0.0	2.8	2.8	2.8	8.0	5.9	15.2	X	X	X
EES	0.2	2.5	2.5	2.5	8.5	20.4	15.9	37.4	55.3	
TES	0.0	3.0	3.0	3.0	7.4	18.0	14.6	38.7		
EES+TES	0.0	3.0	3.0	3.0	8.4	20.0	14.9	31.2	54.7	
Export	0.4	2.8	2.8	2.8	11.9	17.2	19.8	22.7	25.3	27.9
Export w/EES+TES	0.0	3.1	3.1	3.1	10.6	16.0	19.0	21.7	24.2	26.9
EES (MWh)										
EES	3.9	3.6	3.6	3.6	7.8	20.5	27.3	103.4	205.6	X
EES+TES	0.9	0.8	0.8	0.8	4.4	20.8	14.9	52.6	174.3	
Export w/EES+TES	0.9	0.5	0.5	0.5	1.5	1.5	1.2	1.2	1.0	1.0
TES (MWh)										
TES	18.8	7.5	7.5	7.5	21.8	26.7	28.7	211.9	X	X
EES+TES	18.0	4.8	5.0	5.0	7.9	8.8	13.1	57.8	82.0	
Export w/EES+TES	17.8	5.3	5.3	5.3	7.7	6.3	5.9	5.6	5.9	5.7

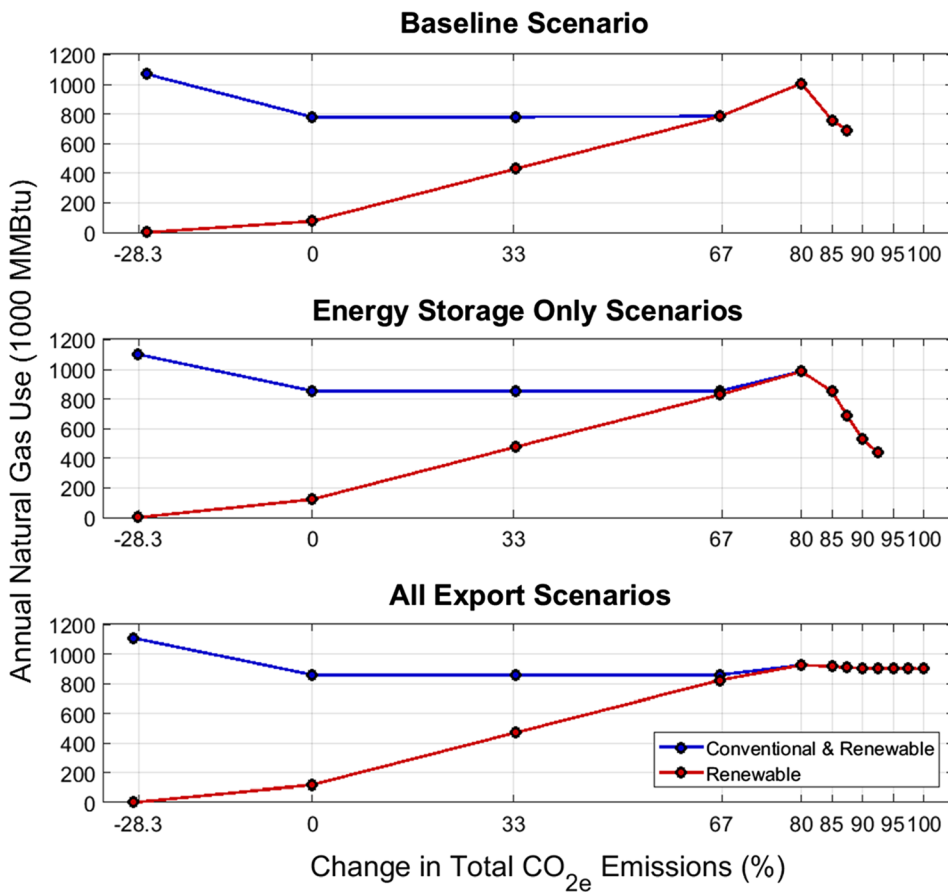


Fig. 4. Optimal annual natural gas use in order to meet the UCI energy demand for all six technology scenarios.

reduced between 0% and 67%.

The optimization results indicate that reducing emissions beyond 67% to 80% requires additional action besides only purchasing renewable fuel. Table 14 shows that the size of the adopted PV system increases, while Fig. 4 and Fig. 5 show that nearly all electricity is produced onsite by the adopted GT, using only renewable fuel. Further reductions result in a divergence in adopted technology between the technology scenarios that allow for export, and those that do not allow for export. For the two scenarios that do allow export to the utility, a GT powered exclusively by renewable fuel is adopted in every scenario, and PV system size increases as emissions are further reduced. Although the share of produced electricity by the GT shrinks as PV system size increases, Fig. 4 suggests that GT operation does not significantly change since fuel consumption remains relatively flat between a reduction of 80% and 100%.

The other four technology scenarios also adopt larger PV systems, and all of these scenarios are required to adopt larger PV systems compared to the export scenarios at the same level of CO_{2e} reduction. In addition, multiple FC systems are adopted in place of the less efficient GT, and overall fuel consumption decreases. This transition from a GT to multiple FCs also results in a decrease in the adopted system size. However, once FCs are adopted, further emissions reductions are achieved only through increasing the PV system size.

Table 14 also shows that for the technology scenarios that include storage, but do not allow for export, energy storage size increases with PV system size.

Only conventional buses are adopted across all technology scenarios, except cases for when CO_{2e} emissions are constrained to be reduced by 85%. At this point, renewable fuel buses are adopted to replace the conventional buses. In the examined scenarios, PEBs were never adopted due to the high capital cost.

4.1. Optimal DER system operation

Although similar DER systems are adopted, and the overall quantity of used fuel and electricity generation by source is similar between the technology scenarios for a CO_{2e} reduction up to 67%, different technology options ultimately result in slightly different optimal operation. For example, Fig. 6 shows electrical operation of the DER systems during two winter weeks when CO_{2e} emissions are unconstrained. Note that operation for all scenarios that include energy storage, but do not allow for export, are similar to the EES + TES scenario, and both scenarios that do allow for export are similar. Please note that in all dispatch plots, the EES charge line is zero whenever no EES charging is occurring, and turns negative whenever EES charging occurs.

Typically, the GT follows the campus demand, resulting in electrical import only when campus demand exceeds the GT capacity. However, during the first Sunday morning shown in Fig. 6, an instance occurs when the campus demand is lower than the minimum allowable GT power output. Under the baseline scenario, the GT is forced to shut down, resulting in a large utility demand and the corresponding demand charges. This is avoided in all other scenarios by operating the GT at the minimum power output. The excess is either exported to the grid if possible, or stored for later use. In addition to supporting GT operation, the adopted storage can be seen as performing both load shifting (during the first Monday) and peak shaving (second Monday). Despite this operation, the relatively small size of the adopted storage results in little impact to the overall load.

When an emissions constraint is initially implemented and increased to a 67% reduction, the adopted GT is operated at part load more often, resulting in greater utility import in the middle of the day (seen in Fig. 7), and renewable natural gas use replaces conventional gas. Note, however, that the GT is operated dynamically in the middle

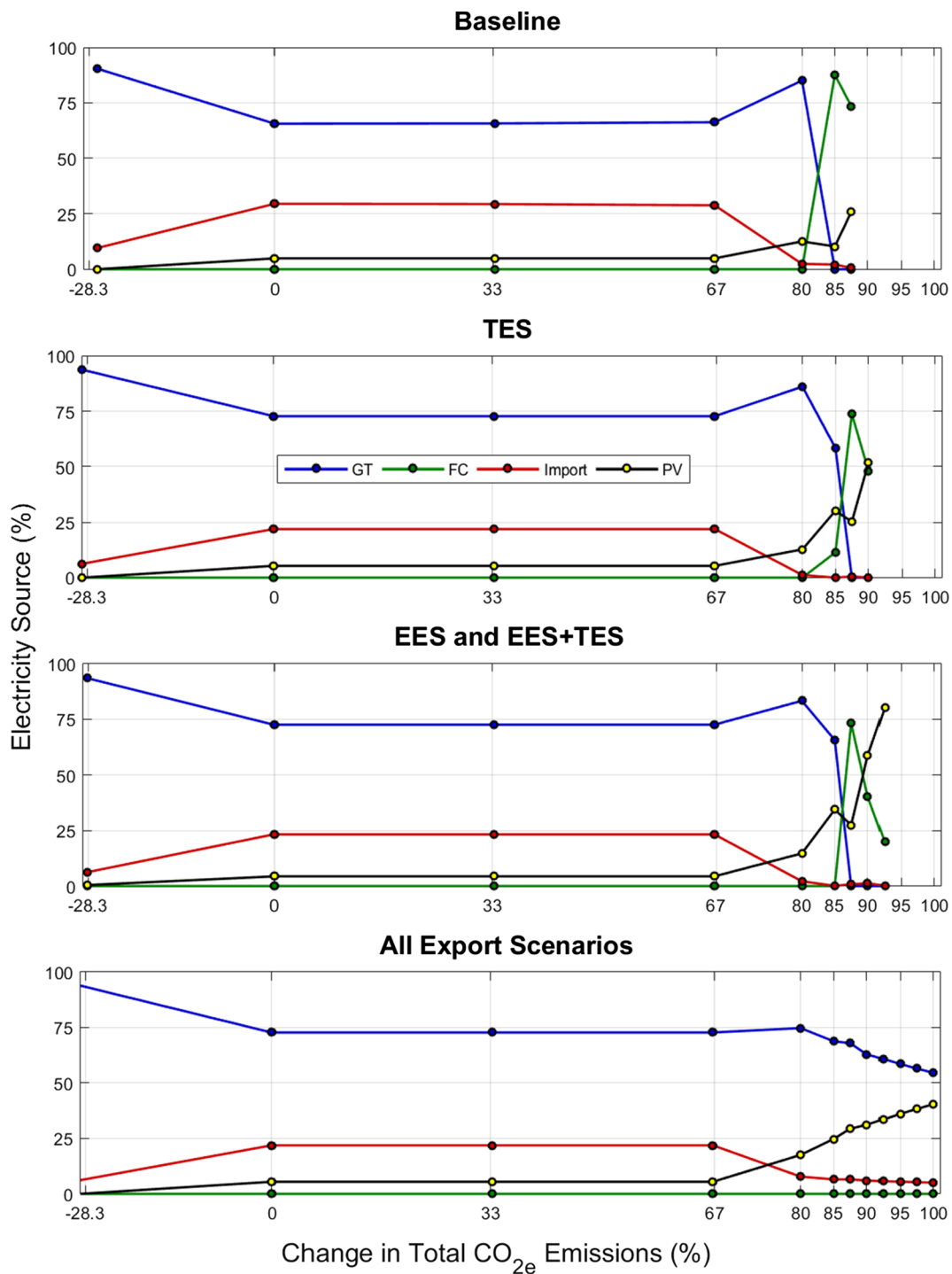


Fig. 5. Electricity source for all technology scenarios and CO₂e emission limits.

of the day more often when energy storage or export is available, indicating that the GT is still capable of economically operating to reduce on-peak energy charges and demand charges.

Operation during the summer mirrors winter operation, with the primary difference being on-peak and mid-peak operation, as shown in Fig. 8. During the summer, the GT performs some load-following during the day to manage peak period demand charges. Under the export scenarios, summer on-peak presents the only instance when GT operation cost less than on-peak export rates, resulting in a direct profit from exporting excess GT production. Also, note for the baseline scenario, that the GT is shut down for a portion of the first Saturday. Since the GT was forced to shut down during the first Sunday, a large demand

charge had already been incurred by the first Saturday. As a result, the GT is shutdown, and PV production is not curtailed.

Whereas a CO₂e reduction of up to 67% can be achieved by a switch from conventional to renewable gas, further CO₂e emissions reductions are accomplished by switching from a GT to a progressively larger PV system, and an FC system if export is not allowed. How the PV affects operation can be split between non-export and export technology scenarios. Although the four scenarios that do not allow export all experience different operation, the general operational trend remains the same; PV is used to supplant any fuel-based energy conversion process.

Operations for the EES + TES technology scenario when emissions are reduced by 80%, 87.5%, and 92.5% is shown in Fig. 9. As the

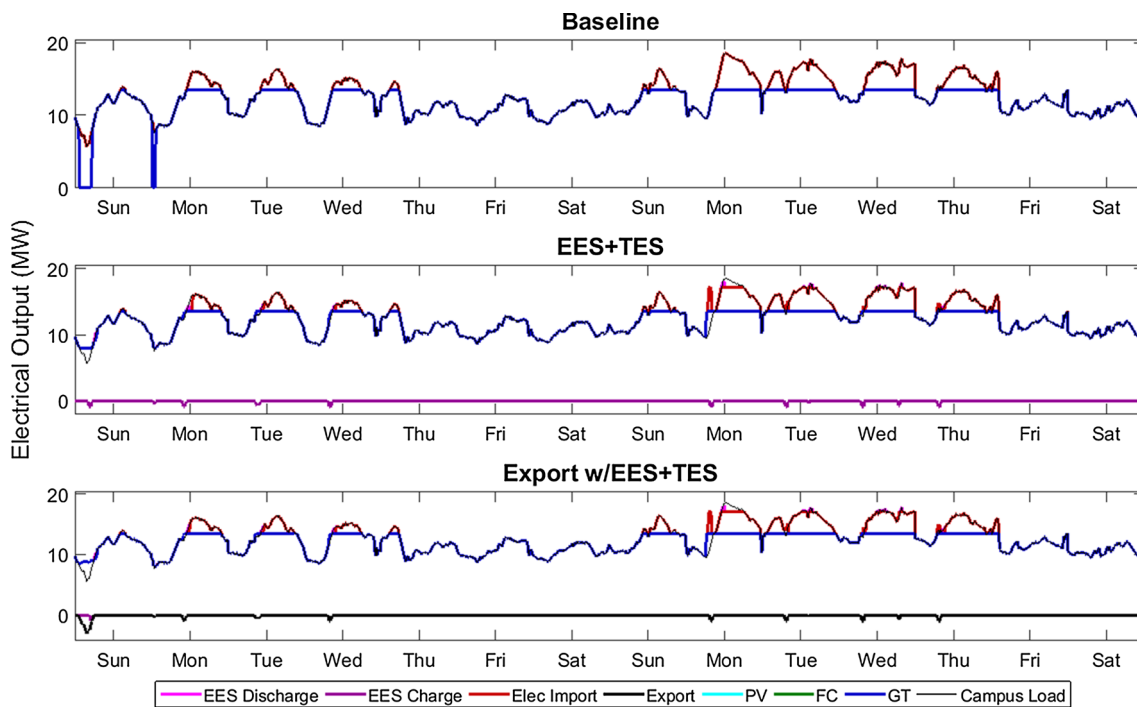


Fig. 6. Electrical operation during two winter weeks for the baseline, EES + TES, and export w/EES + TES technology scenarios, when CO₂e emissions are unconstrained.

emissions constraint shrinks, the GT or FC system are turned down or shut off. In the particular case of the EES + TES technology scenario, reducing CO₂e emissions further is accomplished by using PV to charge an EES, which is subsequently discharged after the sun has set. In this case, the adopted FC system is operated to only meet the energy demand that cannot be met by the EES, with FC operation primarily occurring in the early morning prior to sunrise (as seen in the first week), or when solar resources are limited (as seen in the second week). General operation of the EES only and TES only scenarios mirrors the

EES + TES technology scenario. The baseline technology scenario, however, does not have the ability to store excess PV production for later use. As a result, the adopted PV system exclusively offsets GT and FC operation. For example, in Fig. 9 for a CO₂e emissions reduction of 87.5%, numerous instances exist in the first week where PV production is used to charge the EES, while the FC system remains operational. Under the baseline scenario, FC output would have been reduced, or the system would have been shut down.

While the non-export scenarios experienced a shift in generation

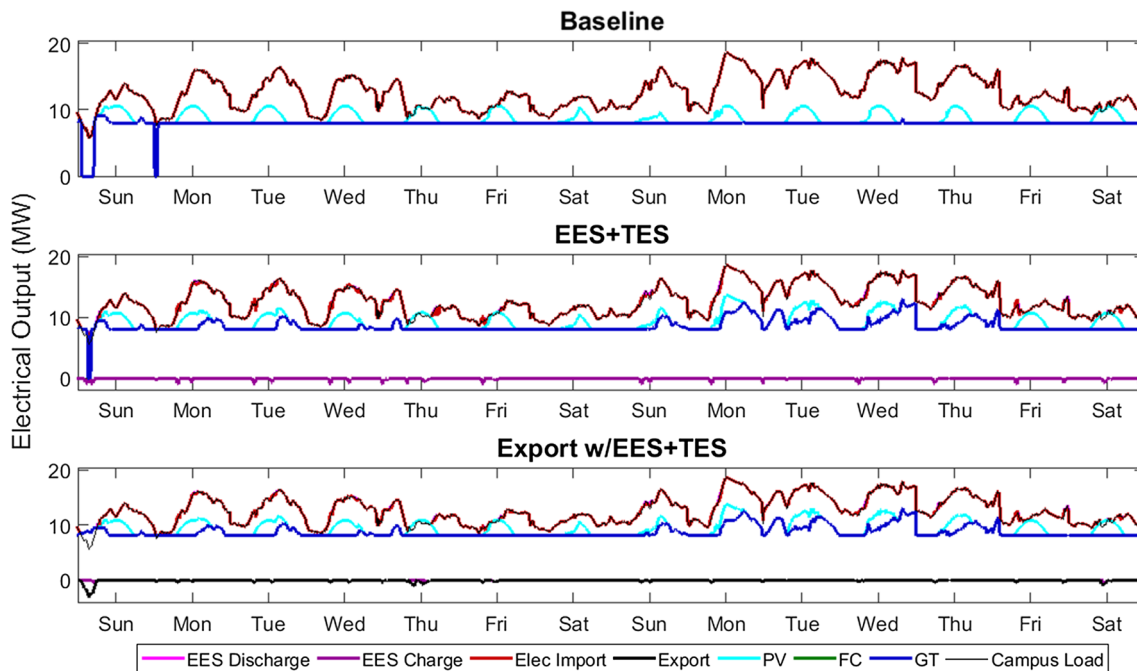


Fig. 7. Electrical operation during two winter weeks for the baseline, EES + TES, and export w/EES + TES technology scenarios, when CO₂e emissions are reduced by between 0% and 67%.

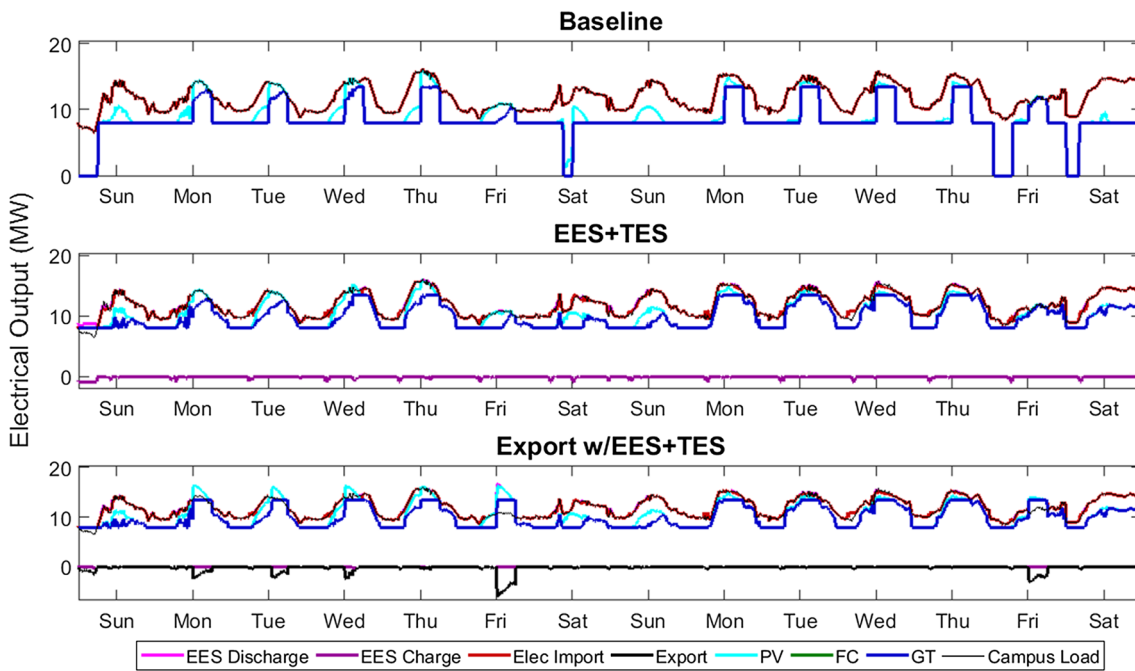


Fig. 8. Electrical operation during two summer weeks for the baseline, EES + TES, and export w/EES + TES technology scenarios, when CO_{2e} emissions are reduced by between 0% and 67%

towards PV, GT operation does not substantially change under the two export scenarios. Winter operation is shown in Fig. 10 for the export w/EES + TES technology scenario when CO_{2e} emissions are reduced by 80%, 90%, and 100%. Qualitatively, export technology scenario operation is nearly identical to export w/EES + TES operation. Since the CO_{2e} constraint also includes avoided emissions due to export back to the grid, and the avoided emissions rate is set by the concurrent average grid emissions rate, a net reduction under the export scenario beyond 67% is achieved by exporting CO_{2e} free electricity back to the utility. When the emissions benefit of exporting excess PV back to the grid is removed, the CO_{2e} reduction for the export and export w/EES + TES technology scenarios is 77% and 78% respectively.

Different types of energy storage operation are seen in Fig. 6

through Fig. 10, including demand shifting and reduction (Fig. 5 and Fig. 8), GT support (Fig. 6 through Fig. 8), and the shifting of PV production to meet night-time demand (Fig. 9 and Fig. 10). Export to the grid is used similarly, with GT support (Fig. 6), on-peak sales back to the grid (Fig. 8), and export of CO_{2e} free energy back to the grid (Fig. 10) all occurring. While the overall impact of adopting storage or exporting back to the grid, the quantity of energy passing through these different paths changes with the system requirements. The percent of overall generation (DER production plus utility imports) that is sent to storage or exported is shown in Table 15. Across the board, the percent of electricity generation that results in storage or export remains low until emissions are reduced by 80% or more. When the required emission reduction is less than 80%, the most effective service provided

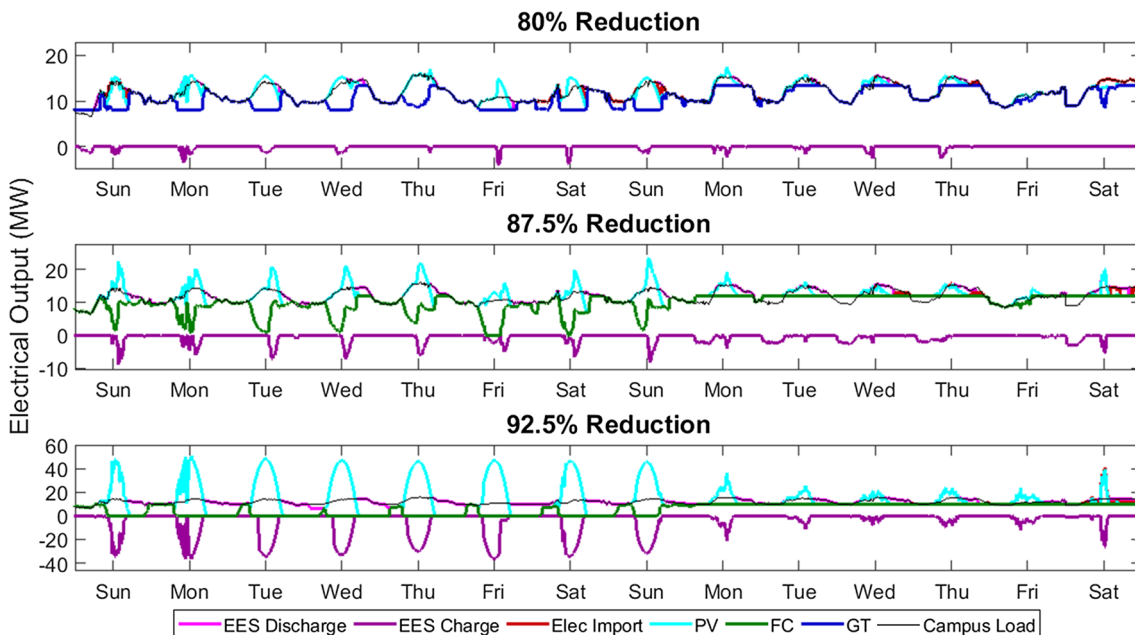


Fig. 9. Operation during two winter weeks for the EES + TES technology scenario when CO_{2e} emissions are reduced by 80%, 85%, and 87.5%

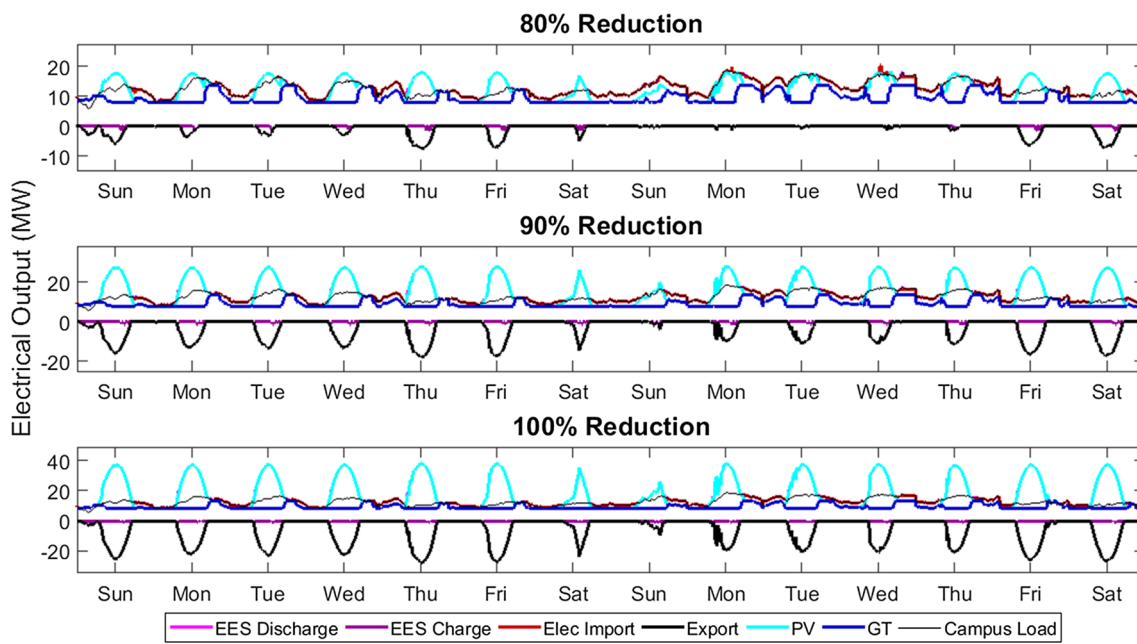


Fig. 10. Operation during two winter weeks for the export w/EES + TES technology scenario when CO_{2e} emissions are reduced by 80%, 90%, and 100%

by storage and export is allowing the GT to stay operational when campus demand is load, avoiding a demand charge associated with approximately 8 MW of utility import. When emissions are reduced by over 80%, storage and export provide a means through which excess PV production can still lead to an emissions reduction, and are not curtailed. In addition, these values appear to follow the percent of energy generated by adopted PV, as seen in Fig. 5. Between an 80% and 90% reduction, approximately one quarter of all PV production is stored or exported. Beyond a 90% reduction, approximately half of all PV production is either stored or exported.

4.2. Investment and emissions reduction costs

Simulation operation and debt cost, as well as the initial investment cost associated with purchasing the optimal DER system is seen in Fig. 11. Since the overall simulation uses three months of data, the operating and debt costs are effectively quarterly costs. Fig. 11 shows

that operating costs experience an initial increase due to the enforcement of a CO_{2e} constraint, resulting in an increase in renewable gas consumption. However, as CO_{2e} emissions are reduced beyond 80%, and generation shifts from GT or FC towards PV, operating costs begin to decrease back to, or below, cost levels set by unconstrained operation. This operating cost benefit, however, is more than offset by increased debt payments due to the adoption of large PV systems (and storage when available). Depending upon the technology scenario, debt cost increases between two and a half to six times from unconstrained levels to the maximum feasible CO_{2e} reduction. In addition, the shift towards PV results in a significantly larger upfront capital expenditure in order to adopt the system. According to the results, allowing export also allows for the DER system adopter to avoid purchasing the large PV and storage system associated with the other technology scenarios, greatly reducing both debt and initial investment cost.

From an investment perspective, the only scenario that performs well is that when CO_{2e} emissions are unconstrained. Under this

Table 15

Percent of generation (on-site DER plus utility imports) that are sent to storage or exported for each technology scenario and level of CO_{2e} reduction.

CO _{2e} Emission Reduction	Percent of Generation Sent to Storage or Exported (%)								
	Technology Scenario		EES	TES	EES+TES		Export	Export w/EES+TES	
	Generation Destination	To EES	To TES	To EES	To TES	To Export	To EES	To TES	To Export
UC	0.9	0.3	0.2	0.2		0.3	0.3	0.2	0.3
0	1.1	0.1	0.4	0.1		0.5	0.2	0.0	0.5
33	1.1	0.1	0.3	0.1		0.5	0.2	0.0	0.5
67	1.1	0.1	0.3	0.1		0.5	0.2	0.0	0.5
80	2.2	0.9	1.3	0.3		7.3	0.5	0.1	5.2
85	6.3	2.1	6.7	0.3		13.8	0.5	0.1	11.9
87.50	7.2	1.5	4.5	0.3		16.9	0.4	0.1	15.1
90	26.0	10.5	14.9	2.3		19.7	0.3	0.0	18.2
92.50	46.4	X	41.6	2.9		22.3	0.3	0.1	21.1
95	X	X	X	X		24.9	0.3	0.0	23.7
97.50	X	X	X	X		27.3	0.3	0.0	26.2
100	X	X	X	X		29.6	0.2	0.0	28.6

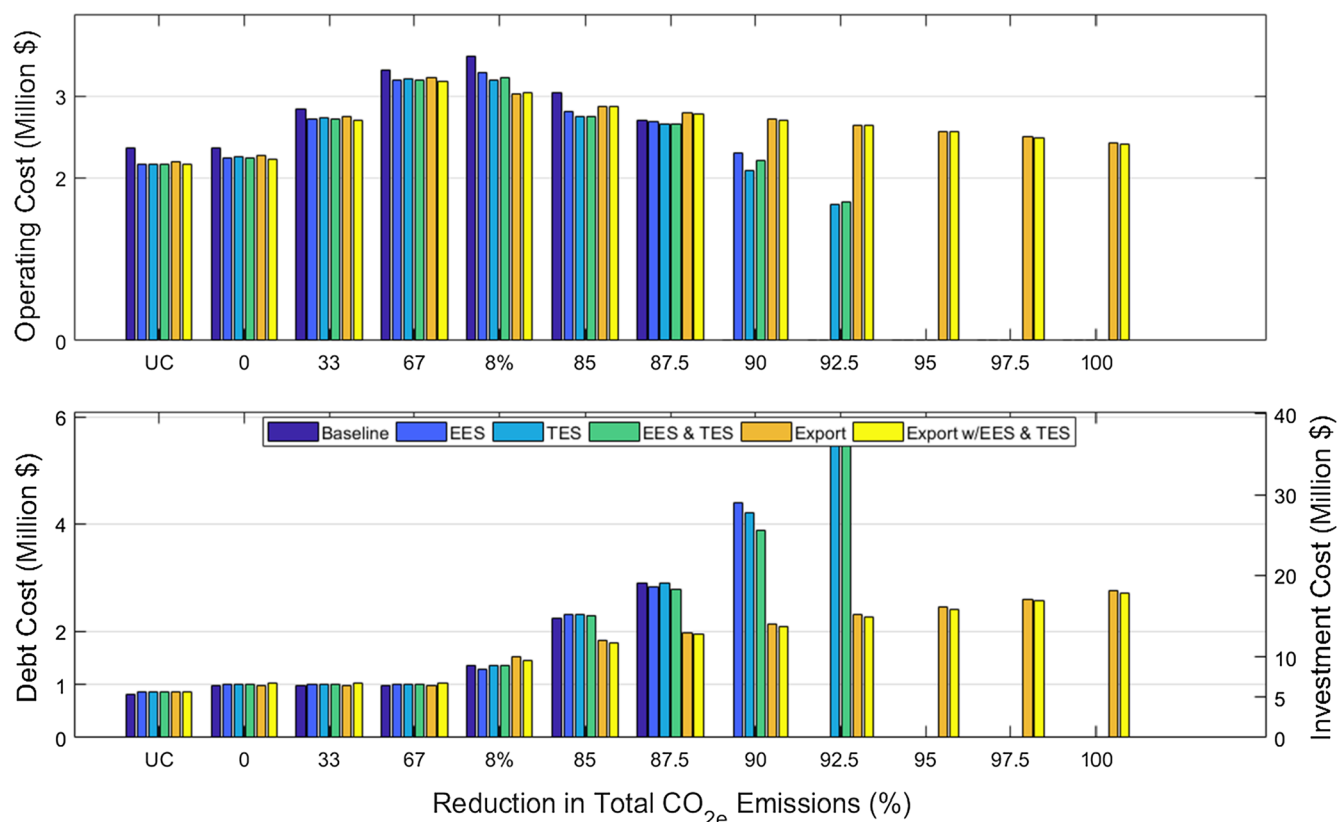


Fig. 11. Quarterly operating and debt costs, and initial investment cost for all six technology scenarios and the six CO_{2e} emission reduction cases tested for the UCI campus.

scenario, the rate of return on DER investment exceeds 20%. Enforcing a 0% increase due to DER investment reduces the rate of return to below 8%, with further reductions eliminating any positive return. This behavior, however, is expected since the competing baseline scenario requires no investment, and provides relatively cheap energy.

Since the goal is to reduce CO_{2e} emissions, it is more effective to judge the investment based on the cost incurred to reduce CO_{2e}

emissions. Fig. 12 shows a simple metric comprised of the additional cost incurred above the baseline cost (campus demand is met by the local utility) divided by the weight of avoided emissions, or dollars per tonne, or, the cost for reducing emissions for each technology scenario. The cost can be split into two regimes; the renewable gas regime, and the solar PV regime. The lowest cost to reduce CO_{2e} is found in the renewable gas regime, where the cost of reducing emissions is primarily

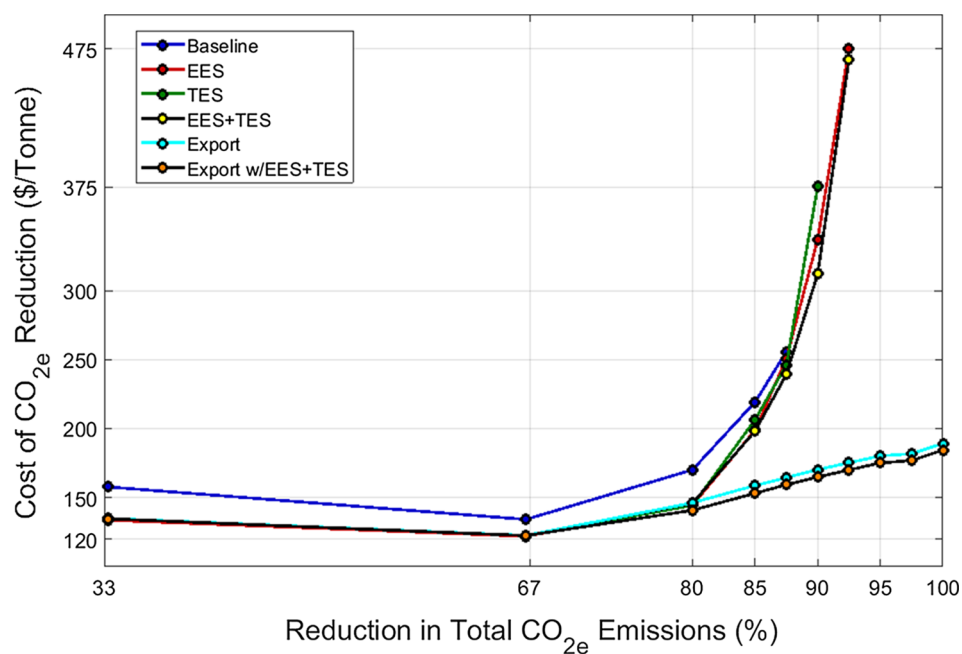


Fig. 12. Cost of CO_{2e} reduction for all technology scenario and CO_{2e} emission limit.

due to the premium associated with the renewable fuel. Within this regime, the baseline technology scenario has the highest cost due to the inflexible response of the DER system to low campus energy demand, and the addition of energy storage and export capabilities are mainly associated with increased operational flexibility.

Within the PV regime, the addition of storage allows for CO_{2e} emissions to be reduced further than possible in the baseline case. However, a larger solar PV array is required under these scenarios, resulting in a much higher cost than when unlimited export. This difference in savings between export and all other scenarios approaches \$300 per tonne when emissions are reduced by 90%. As expected, the scenario with the greatest number of options (Export w/EES + TES) achieves the lowest cost.

It is important to note that another driver in this result is the assumption that exported electricity can reduce CO_{2e} emissions at the average grid emissions rate. When export is not allowed, solar PV production is used to replace GT or FC operation fueled with renewable natural gas. As a result, under the current methodology, any export of solar PV to offset CO_{2e} emissions is considered to have a greater effect than being stored for later use onsite...

4.3. Export with wholesale rates

The results presented in the preceding sections were determined while assuming that all electricity exported back to the utility was sold at near retail rates. As discussed in [Section 3](#), retail rates, or Net Energy Metering rates, typically only apply to the amount of exported electricity equal to the amount of imported electricity. This assumption appears to be valid for the two export scenarios up until CO_{2e} emissions are reduced by more than 80%. At this point, further emissions reductions are achieved by purchasing a larger PV system, and exporting excess electricity back to the grid. When emissions are reduced by 85%, the resulting export is 1.6 times greater than the total import for the export scenario, and 1.8 times greater under the export w/EES + TES scenario. When emissions are reduced by 100%, these values jump to 4.4 and 5.6 for export and export w/EES + TES respectively. Clearly, a large portion of exported electricity in these scenarios will not be sold back to the grid at retail rates, but at wholesale rates.

In order to test the effect of exporting electricity at a reduced rate, the optimization model was run for both export scenarios with an export price of \$0.03 and \$0 per kWh. The results show, that in general, a GT and similarly sized HRU are always adopted, regardless of CO_{2e} emissions reduction constraint. In addition, there was virtually no difference in both DER adoption and operation between an export price of \$0.03 and \$0 per kWh for all levels of CO_{2e} emissions reduction.

When emissions are reduced by less than 80%, similarly sized PV and storage systems are adopted, and unnecessary export when excess GT capacity exists is eliminated (as shown in [Fig. 8](#)). Reducing emissions by 80% or more does result in a change in PV and energy storage adoption, as well as DER system operation. The percent difference in adopted PV and storage systems for the export and export w/EES + TES technology scenarios between NEM and wholesale optimization results is shown in [Table 16](#). According to these results, solar PV capacity decreases with the reduced export price, and energy storage tends to increase. Note that despite the large increase in system size, the storage requirements when export is available is much lower than any storage only scenario.

The decrease in PV system size is coupled with a decrease in utility imports. Referring to [Fig. 5](#), a small percentage of energy procurement for the export scenarios still came from utility imports. Under wholesale rates, this import is eliminated, and met through either increasing GT output, or by adopting larger storage to shift PV production to meet later demand.

As expected, the cost of reducing emissions increases as a result of decreasing the export price, as shown in [Fig. 13](#). This increase, however, is only noticeable when emissions are reduced by 85% or more.

Within this range, further emission reductions are achieved through the export of excess PV production, resulting in a cost increase of up to \$19 per tonne under \$0.03 per kWh rates, and \$40 per tonne under \$0 per kWh rates. Note that, even when excess PV production is provided back to the grid for free, the cost to reduce CO_{2e} is still lower than the closest non-export technology scenario.

4.4. Sensitivity of Results to Fuel Cell Capital Cost

According to the optimization results presented in [Table 13](#), FC systems are not adopted until emissions are reduced by 85% or more. In addition, FCs are never adopted in any scenario that allows for export. This result can be almost completely attributed to the assumed capital cost of \$4000 per kW of FC capacity. While this cost may be accurate for some current fuel cell systems, the optimization does not take into account possible economies of scale that may be realized when installing large FC systems. Depending on the possibility of combining balance of plant components and the additional construction required to install a fuel cell plant, it is possible to achieve a cost lower than \$4000 per kW. Instead of conducting an extensive analysis to determine costs at which FC adoption becomes desirable, the current optimization was run with a progressively lower FC capital cost until adoption occurred, and the GT was replaced by a FC system. Since FC adoption never occurred when export is allowed, the export technology scenario was used to test for FC adoption. Note that these results are relative to the \$1400 per kW for the GT, and \$2000 per kW for PV. FC system adoption occurs in the scenarios considered at the following FC system prices: \$1500 per kW when emissions are unconstrained, \$2000 per kW when emissions are reduced by 0%, \$2200 per kW when reduced by 33%, \$2250 when reduced by 67%, \$2800 when reduced by 80%, and \$3000 when reduced by between 85% and 100%.

5. Analysis

The current study shows an optimal DER adoption trajectory for each technology scenario for reducing CO_{2e} emissions. For all scenarios, the first course of action is to adopt a conventional CHP generator, and to fuel the purchased generator using renewable fuel. Once the maximum CO_{2e} reduction through CHP has been realized, PV is to be adopted, preferably with the ability to export excess production back to the grid. If export is not allowed, emissions can still be reduced by 85%. However, further emissions reductions can only be achieved if storage is also adopted. This work did not provide a method for decarbonizing heating demand other than through the use of CHP and the burning of renewable gas. If export is not allowed, additional technologies associated with the production of heat must be included if net CO_{2e} emissions are to be reduced by 100%.

In terms of both actual cost and cost of reducing emissions, there is

Table 16

Change to adopted PV and storage capacities as a result of optimizing for wholesale export rates versus NEM rates.

Emission Reduction (%)	Percent Difference Between NEM and Wholesale Results			
	Export	Export w/EES + TES		
		PV	EES	TES
80	−25.3	−12.2	101.9	26.2
85	−22.8	−15.6	70.9	−24.9
87.5	−18.6	−14.5	76.5	−2.7
90	−16.9	−12.5	71.6	2.6
92.5	−14.8	−10.6	103.5	8.8
95	−13.1	−9.6	93.1	17.1
97.5	−11.9	−8.6	76.2	27.3
100	−10.8	−7.8	82.5	29.6

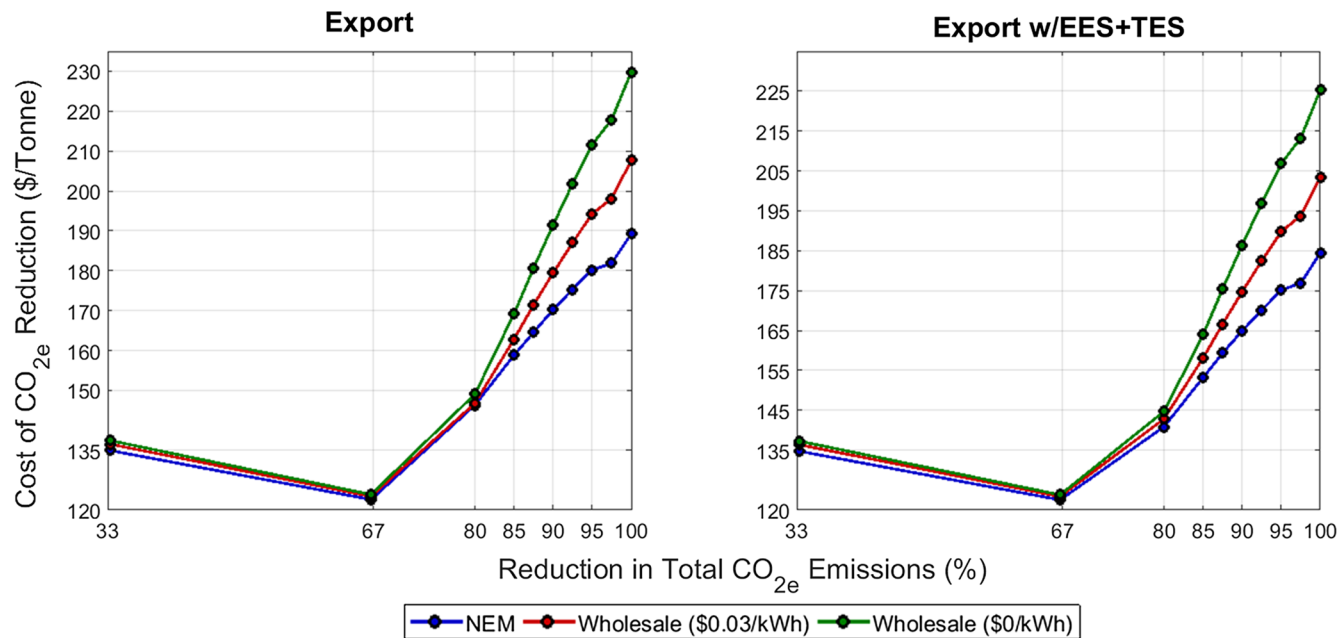


Fig. 13. Cost of CO_{2e} reduction for both export technology scenarios under NEM and wholesale (\$0.03/kWh and \$0 per kWh) export rates.

little difference between the technology scenarios until emissions are reduced beyond the point of what is capable through the use of renewable gas in a conventional CHP system (85% reduction). Until this point, the value created by storage and export is not associated with lowering emissions, but with creating operational flexibility. The optimization results clearly show that export and storage are not extensively used in a manner that reduces emissions until a large PV system is required. Prior to this regime, the storage size decreases as a result of reducing emissions. This signifies that the typical value associated with storage (demand shifting and reduction) does not outweigh the increase in CO_{2e} emissions due to a round trip efficiency less than 100%. Within this same range of CO_{2e} emissions reduction (less than 80%), export of electricity during peak periods may still occur, but only if the overall cost of energy conversion (including the cost of renewable gas) is less than the price to export.

While these results indicate that export is critical to maintaining low cost while achieving deep carbon emissions reductions, the optimization formulation does not account for local grid impacts, or how utility assets would be operated differently due to customer export. In addition, the optimization formulation does not take into account local grid infrastructure constraints. Despite these issues, the results of this work support the development and upgrade of the current electric grid as a means to enable the effective trading of excess solar power. If improved infrastructure were to be combined with a more realistic avoided emissions rate that considers the overall impact of exported power, then excess solar production could be more effectively deployed with storage technologies to offset the most CO_{2e} intensive generators. Such an improvement is likely to support the adoption of PV, while also encouraging the adoption and operation of storage such that the maximum environmental benefit is realized.

Interestingly, the export scenarios maintain the lowest cost of CO_{2e} reduction cost when the export price is reduced to zero. Note that these scenarios do not, however, consider any costs associated with the utility infrastructure investments that may be required to allow export. At such high levels of emission reduction, the DER operator is essentially entering the business of generating electricity with the sole purpose of delivery to the grid. In fact, a large portion of the adopted PV power at emission reductions greater than 85% does not interact with the campus electrical demand, or any available storage devices. If the excess electricity is provided back to the grid for free, then the DER

adopter is essentially paying \$0.15 per kWh for the ability to export back to the grid. Using the average grid emissions factor of 295 kg/MWh, this corresponds to the DER operator paying approximately \$515 per tonne of avoided CO_{2e} emissions.

As presented, the results regarding export are similar to the results on the use of renewable gas; both present a solution that is only viable for early adopters. For export, local grid infrastructure and reliability constraints will limit the amount of export that can occur within any portion of a utility distribution system. For fuel use, even if the full renewable biogas and biomass fuel potential in the United States were realized, renewable gas can only meet a fraction of the total fuel demand [58]. In this case, the use of export and renewable biogas as presented in this work can only be possible for the first adopters, as the resources associated with these behaviors (current grid infrastructure for export, and proper feedstock for renewable gas) are limited. The results are not extensible to society at large, since sufficient biogas resources are not available. In these scenarios, the cost of between \$120 and \$200 per tonne of CO_{2e} emissions reduced is the cost floor for reducing CO_{2e} in California. If CO_{2e} emissions across society are reduced, then the actual cost to reduce emissions is likely to follow the curve established by the non-export technology scenarios. However, if renewable hydrogen gas (or renewable methane as produced from renewable hydrogen and captures carbon dioxide by methanation) was to be considered as produced in support of higher renewable use in society (e.g., by electrolysis of water using otherwise curtailed renewable power), then, renewable gas use could become ubiquitous and unbounded by the availability of biogas and biomass resources. The utility grid network coupled and integrated nature of producing renewable gas in this fashion is a matter that requires additional study.

It is important to acknowledge the power grid in California is relatively clean, making it difficult to reduce CO_{2e} emissions in comparison to purchased grid electricity. If the same resources were to be used in a different part of the United States, then the mass of avoided CO_{2e} emissions could easily double or triple. In certain areas, the adoption and operation of a natural gas-fired CHP system would result in a large reduction in CO_{2e} emissions. However, it is difficult to predict what the cost to reduce CO_{2e} would become in these cases because, while utility emission rates would be higher, the cost of utility electricity, and baseline cost for DER adoption, are also typically lower.

Finally, Fig. 12 presents costs to reduce emissions that are much

higher than current costs that are typically experienced in carbon emissions markets. Today, a permit to emit CO_{2e} can be purchased at less than \$15 per metric ton [59]. This value, and the cost values presented in Fig. 12 represent different ideas. While the permit allows for CO_{2e} to be emitted, the values presented in this work represent the cost to eliminate the same amount of CO_{2e}. The presented work is specific to the use of financial assets to purchase renewable gas and/or solar PV, and storage systems, for a university campus. It does not account for the use of the same technical and financial resources in different ways that may reduce emissions further than presented in this work. However, this work does show that, if the goal of selling CO_{2e} permits is to eventually reduce emissions, the current cost of CO_{2e} must be increased.

6. Summary and conclusion

This work examines how a DER system can be optimally designed and operated to minimize cost of energy while reducing greenhouse gas emissions (considered in terms of equivalent amount of CO_{2e} emissions) in the state of California. The DER optimization problem was formulated as a mixed integer linear program that included a novel formulation of a declining block utility natural gas rate structure, DG minimum on/off time requirements, TES constraint coefficients, and interactions with a bus system. The model, known as DERopt, optimized a DER system that included solar PV, renewable gas, and the ability to export electricity, such that CO_{2e} emissions were reduced by a specified (constrained) amount. Six technology scenarios were designed for varying levels of carbon emissions reduction for the University of California, Irvine in order to examine if a trajectory of DER adoption exists, and to determine how the different systems respond when required to emit less CO_{2e}. The main findings of this analysis are:

- When available, the least expensive way to reduce CO_{2e} emissions is through the use of renewable gas with a conventional generator, such as a gas turbine, with waste heat recovery. Assuming the costs used in this work, it can cost between \$150 and \$120 per metric ton of CO_{2e} reduced.
- Reducing emissions beyond what is possible through the use of renewable gas required the adoption of a progressively larger solar PV system. As the size of the solar PV system increased, so did the cost to reduce emissions. The cost to reduce emissions by 85% for the scenarios examined in this work reached a maximum of \$475 per metric ton of CO_{2e}. Allowing for energy storage technology allowed for a smaller PV system to be adopted, reducing the cost of CO_{2e} emissions reductions to nearly \$300 per metric ton. Allowing export with storage reduced the cost even further to below \$200 per metric ton.
- When export is allowed, the rate at which electricity is sold back to the grid appears to have little to no effect on DER adoption and operation when emissions are reduced by up to 80%. Decreasing emissions by greater than 80% under wholesale rates results in a decrease in PV size adoption by 25%, and, when allowed, an increase in EES adoption by 70% to 100%. Export of excess PV is reduced, utility imports are virtually eliminated, and GT operation increases. Little difference was found between results produced with an export price of \$0.03 and \$0 per kWh. Despite the reduced value, export under wholesale rates provides the lowest cost path to achieving zero net CO_{2e} emissions.
- Once the emissions reductions provided by using only renewable gas have been achieved, the method through which additional reductions can be achieved depends upon available options. When no storage or export is available, more efficiency generators, such as fuel cells, must be adopted. When storage is available, conventional generators are kept, and the storage is used to shift solar production to meet energy demand during the evening and night. When export is available, excess solar generation is sold back to the grid to replace the production of electricity from fossil fuel power plants.

- When considering a bus system, other options (such as solar PV) are always preferred by the optimization first, due to the high cost of electric buses.

Acknowledgment

The authors gratefully acknowledge University of California Office of the President for partial funding support of this effort under the Carbon Neutrality Initiative and the contributions of contract manager Rob Judd.

References

- [1] University of California. Carbon Neutrality Initiative | UCOP 2013. <http://www.ucop.edu/initiatives/carbon-neutrality-initiative.html> [accessed June 9, 2016].
- [2] Pavley F, Nunez F. California Assembly Bill No. 32-Global Warming Solutions Act of 2006. vol. 5. 2006.
- [3] Naimaster EJ, Sleiti AK, Naimaster IV EJ, Sleiti AK. Potential of SOFC CHP systems for energy-efficient commercial buildings. Energy Build 2013;61:153–60. <https://doi.org/10.1016/j.enbuild.2012.09.045>.
- [4] Nanaeda K, Mueller F, Brouwer J, Samuelsen S. Dynamic modeling and evaluation of solid oxide fuel cell – combined heat and power system operating strategies. J Power Sources 2010;195:3176–85. <https://doi.org/10.1016/j.jpowsour.2009.11.137>.
- [5] Flores Shaffer BP, Brouwer JRJ, Flores RJ, Shaffer BP, Brouwer J. Economic and sensitivity analyses of dynamic distributed generation dispatch to reduce building energy cost. Energy Build 2014;85:293–304. <https://doi.org/10.1016/j.enbuild.2014.09.034>.
- [6] Flores RJ, Shaffer BP, Brouwer J, Flores Shaffer BP, Brouwer JRJ. Dynamic distributed generation dispatch strategy for lowering the cost of building energy. Appl Energy 2014;123:196–208. <https://doi.org/10.1016/j.apenergy.2014.02.028>.
- [7] Medrano M, Brouwer J, McDonell V, Mauzey J, Samuelsen S. Integration of distributed generation systems into generic types of commercial buildings in California. Energy Build 2008;40:537–48.
- [8] Knizley AA, Mago PJ, Smith AD. Evaluation of the performance of combined cooling, heating, and power systems with dual power generation units. Energy Policy 2014;66:654–65. <https://doi.org/10.1016/j.enpol.2013.11.017>.
- [9] Pruitt KA, Braun RJ, Newman AM. Establishing conditions for the economic viability of fuel cell-based, combined heat and power distributed generation systems. Appl Energy 2013;111:904–20.
- [10] Fang F, Wang QH, Shi Y. A novel optimal operational strategy for the CCHP system based on two operating modes. Power Syst IEEE Trans 2012;27:1032–41. <https://doi.org/10.1109/TPWRS.2011.2175490>.
- [11] Wang H, Yin W, Abdollahi E, Lahdelma R, Jiao W. Modelling and optimization of CHP based district heating system with renewable energy production and energy storage. Appl Energy 2015;159:401–21. <https://doi.org/10.1016/j.apenergy.2015.09.020>.
- [12] Ruan Y, Liu Q, Li Z, Wu J. Optimization and analysis of Building Combined Cooling, Heating and Power (BCHP) plants with chilled ice thermal storage system. Appl Energy 2016;179:738–54. <https://doi.org/10.1016/j.apenergy.2016.07.009>.
- [13] Lozano MA, Carvalho M, Serra LM. Operational strategy and marginal costs in simple trigeneration systems. Energy 2009;34:2001–8. <https://doi.org/10.1016/j.energy.2009.08.015>.
- [14] Hu M, Cho H. A probability constrained multi-objective optimization model for CCHP system operation decision support. Appl Energy 2014;116:230–42. <https://doi.org/10.1016/j.apenergy.2013.11.065>.
- [15] Collazos A, Maréchal F, Gähler C. Predictive optimal management method for the control of polygeneration systems. Comput Chem Eng 2009;33:1584–92. <https://doi.org/10.1016/j.compchemeng.2009.05.009>.
- [16] Bozchalui MC, Sharma R. Optimal operation of commercial building microgrids using multi-objective optimization to achieve emissions and efficiency targets. 2012 IEEE Power Energy Soc. Gen. Meet., IEEE; 2012, p. 1–8. doi:10.1109/PESGM.2012.6345600.
- [17] Ho WS, Macchietto S, Lim JS, Hashim H, Muis ZA, Liu WH. Optimal scheduling of energy storage for renewable energy distributed energy generation system. Renew Sustain Energy Rev 2016;58:1100–7. <https://doi.org/10.1016/j.rser.2015.12.097>.
- [18] Keirstead J, Samsatli N, Shah N, Weber C. The impact of CHP (combined heat and power) planning restrictions on the efficiency of urban energy systems. Energy 2012;41:93–103. <https://doi.org/10.1016/j.energy.2011.06.011>.
- [19] Yang Y, Zhang S, Xiao Y. Optimal design of distributed energy resource systems coupled with energy distribution networks. Energy 2015;85:433–48. <https://doi.org/10.1016/j.energy.2015.03.101>.
- [20] Lozano MA, Ramos JC, Serra LM. Cost optimization of the design of CHCP (combined heat, cooling and power) systems under legal constraints. Energy 2010;35:794–805. <https://doi.org/10.1016/j.energy.2009.08.022>.
- [21] Liu P, Gerogiorgis DI, Pistikopoulos EN. Modeling and optimization of poly-generation energy systems. Catal Today 2007;127:347–59. <https://doi.org/10.1016/j.cattod.2007.05.024>.
- [22] Tian Z, Niu J, Lu Y, He S, Tian X. The improvement of a simulation model for a distributed CCHP system and its influence on optimal operation cost and strategy. Appl Energy 2016;165:430–44. <https://doi.org/10.1016/j.apenergy.2015.11.086>.
- [23] Bracco S, Dentici G, Siri S. DESOD : a mathematical programming tool to optimally

- design a distributed energy system. *Energy* 2016;100:298–309. <https://doi.org/10.1016/j.energy.2016.01.050>.
- [24] Wakui T, Yokoyama R. Optimal structural design of residential cogeneration systems with battery based on improved solution method for mixed-integer linear programming. *Energy* 2015;84:106–20. <https://doi.org/10.1016/j.energy.2015.02.056>.
- [25] Liu P, Pistikopoulos EN, Li Z. An energy systems engineering approach to the optimal design of energy systems in commercial buildings. *Energy Policy* 2010;38:4224–31.
- [26] Li L, Mu H, Li N, Li M. Economic and environmental optimization for distributed energy resource systems coupled with district energy networks. *Energy* 2016;109:947–60. <https://doi.org/10.1016/j.energy.2016.05.026>.
- [27] Morvaj B, Evins R, Carmeliet J. Optimization framework for distributed energy systems with integrated electrical grid constraints. *Appl Energy* 2016;171:296–313. <https://doi.org/10.1016/j.apenergy.2016.03.090>.
- [28] Omu A, Hsieh S, Orehoung K. Mixed integer linear programming for the design of solar thermal energy systems with short-term storage. *Appl Energy* 2016;180:313–26. <https://doi.org/10.1016/j.apenergy.2016.07.055>.
- [29] Siddiqui AS, Marnay C, Bailey O, Hamachi La Comaire K. *Optimal selection of on-site generation with combined heat and power applications* 2004.
- [30] Marnay C, Venkataraman G, Stadler M, Siddiqui AS, Firestone R, Chandran B. Optimal technology selection and operation of commercial-building microgrids. *Power Syst IEEE Trans* 2008;23:975–82. <https://doi.org/10.1109/tpwrs.2008.922654>.
- [31] Stadler M, Groissböck M, Cardoso G, Marnay C. Optimizing Distributed Energy Resources and building retrofits with the strategic DER-CAModel. *Appl Energy* 2014;132:557–67. <https://doi.org/10.1016/j.apenergy.2014.07.041>.
- [32] Stadler M, Kloess M, Groissböck M, Cardoso G, Sharma R, Bozchalui MC, et al. Electric storage in California's commercial buildings. *Appl Energy* 2013;104:711–22.
- [33] Milan C, Stadler M, Cardoso G, Mashayekh S. Modeling of non-linear CHP efficiency curves in distributed energy systems. *Appl Energy* 2015;148:334–47. <https://doi.org/10.1016/j.apenergy.2015.03.053>.
- [34] Braslavsky JH, Wall JR, Reedman LJ. Optimal distributed energy resources and the cost of reduced greenhouse gas emissions in a large retail shopping centre. *Appl Energy* 2015;155:120–30. <https://doi.org/10.1016/j.apenergy.2015.05.085>.
- [35] Cardoso G, Stadler M, Bozchalui MC, Sharma R, Marnay C, Barbosa-Póvoa A, et al. Optimal investment and scheduling of distributed energy resources with uncertainty in electric vehicle driving schedules. *Energy* 2014;64:17–30. <https://doi.org/10.1016/j.energy.2013.10.092>.
- [36] Steen D, Stadler M, Cardoso G, Groissböck M, DeForest N, Marnay C. Modeling of thermal storage systems in MILP distributed energy resource models. *Appl Energy* 2015;137:782–92. <https://doi.org/10.1016/j.apenergy.2014.07.036>.
- [37] Mashayekh S, Stadler M, Cardoso G, Heleno M. A mixed integer linear programming approach for optimal DER portfolio, sizing, and placement in multi-energy microgrids. *Appl Energy* 2017;187:154–68. <https://doi.org/10.1016/j.apenergy.2016.11.020>.
- [38] Zeng R, Li H, Liu L, Zhang X, Zhang G. A novel method based on multi-population genetic algorithm for CCHP-GSHP coupling system optimization. *Energy Convers Manage* 2015;105:1138–48. <https://doi.org/10.1016/j.enconman.2015.08.057>.
- [39] Li L, Mu H, Gao W, Li M. Optimization and analysis of CCHP system based on energy loads coupling of residential and office buildings. *Appl Energy* 2014;136:206–16. <https://doi.org/10.1016/j.apenergy.2014.09.020>.
- [40] Pruitt KA, Braun RJ, Newman AM. Evaluating shortfalls in mixed-integer programming approaches for the optimal design and dispatch of distributed generation systems. *Appl Energy* 2013;102:386–98. <https://doi.org/10.1016/j.apenergy.2012.07.030>.
- [41] University of California. Largest university solar power project pushes UC toward carbon neutrality | University of California 2016. <http://universityofcalifornia.edu/news/uc-surges-toward-carbon-neutrality-largest-solar-power-purchase> [accessed July 9, 2016].
- [42] Energy - UC Irvine Sustainability n.d. <http://sustainability.uci.edu/sustainablecampus/energy/>.
- [43] Do AT. *Performance and Controls of Gas Turbine-Driven Combined Cooling Heating and Power Systems for Economic Dispatch*. Irvine: University of California; 2013.
- [44] Hack R. UC Irvine's Combined Heat & Power Plant "A Study in Plant Integration" 2012. <https://www.aeesocal.org/docs/chapterMeeting/44-uc-irvine's-combined-heat-power-plant.pdf> [accessed August 9, 2016].
- [45] Domínguez-Muñoz F, Cejudo-López JM, Carrillo-Andrés A, Gallardo-Salazar M. Selection of typical demand days for CHP optimization. *Energy Build* 2011;43:3036–43. <https://doi.org/10.1016/j.enbuild.2011.07.024>.
- [46] Anteater Express | Home 2008. <http://www.shuttle.uci.edu/> [accessed August 9, 2016].
- [47] Flores RJ. Control of dispatch dynamics for lowering the cost of distributed generation in the built environment; 2013.
- [48] EPA. eGRID2012 Summary Tables. Clean Air Mark Div Off Atmos Programs. US Environ Prot Agency 2015:3–8. <https://doi.org/10.1073/pnas.0703993104>.
- [49] California Independent Systems Operator n.d. <http://www.caiso.com/Pages/default.aspx> [accessed July 7, 2018].
- [50] Flores RJ. *Costs and Operating Dynamics of Integrating Distributed Energy Resources in Commercial and Industrial Buildings with Electric Vehicle Charging*. Irvine: University of California; 2016.
- [51] National Renewable Energy Laboratory. Wind Maps | Geospatial Data Science | NREL n.d. <https://www.nrel.gov/gis/wind.html> [accessed July 7, 2018].
- [52] Important White D. *Factors for Early Market Microgrids: Demand Response and Plug-in Electric Vehicle Charging*. Irvine: University of California at; 2016.
- [53] Southern California Edison. Schedule TOU-8-S TIME-OF-USE - GENERAL SERVICE - LARGE STANDBY 2014. <https://www.sce.com/NR/sc3/tm2/pdf/CE334.pdf>.
- [54] Flores R, Brouwer J. Optimal Design of a Distributed Energy Resources System That Minimizes Cost While Reducing Carbon Emissions. ASME 2017 11th Int Conf Energy Sustain 2017.
- [55] Williams HP. *Model Building in Mathematical Programming*. Wiley; 1999.
- [56] Southern California Edison. Schedule NEM: NET ENERGY METERING 2015. <https://www.sce.com/NR/sc3/tm2/pdf/ce158-12.pdf> [accessed January 1, 2016].
- [57] Southern California Edison. Net Surplus Compensation Rate | Rates & Pricing Choices | SCE Tariff Book | Regulatory Information | Home - SCE 2017. <https://www.sce.com/wps/portal/home/regulatory/tariff-books/rates-pricing-choices/net-surplus-compensation> [accessed January 8, 2017].
- [58] Saur G, Milbrandt A. Renewable Hydrogen Potential from Biogas in the United States Renewable Hydrogen Potential from Biogas in the United States; 2014.
- [59] California Carbon Dashboard: Carbon Prices, the Latest News, and California Policy n.d. <http://calcarbondash.org/> [accessed January 5, 2016].